



NTNU – Trondheim
Norwegian University of
Science and Technology

Bypass Pigging of Subsea Pipelines Suffering Wax Deposition

Tore Galta

Subsea Technology

Submission date: June 2014

Supervisor: Jon Steinar Gudmundsson, IPT

Norwegian University of Science and Technology
Department of Petroleum Engineering and Applied Geophysics

MASTER THESIS
Spring 2014
for stud. techn. Tore Galta

PIPELINES SUFFERING WAX DEPOSITION

Work has been carried out to evaluate the effect of several parameters on the wax thickness profile in a subsea pipeline (Galta 2013). The parameters investigated were flow velocity, inlet temperature, overall heat transfer coefficient, water-cut and time. Results were obtained using the Hysys processing software. Several interesting results were obtained/illustrated, even though simplifying assumptions were used.

In further work (master's thesis) the above parameters will be investigated, but in greater detail. For example, the overall heat transfer coefficient was assumed constant, but in reality it changes with flow velocity and temperature. An oil composition based on Norne crude was used/constructed (actual composition not available). The main aim of the planned master's thesis is to find out how best (optimize) to carry out pigging operations to remove deposited paraffin wax. The following aspects need to be addressed:

- Use overall heat transfer coefficient based on standard correlations for heat transfer coefficients in pipes (varies with flow velocity and temperature)
- Consider what methods can be used to monitor build-up of wax in pipelines
- Model (analytically and using processing software) total pressure drop with evenly distributed wax layer and local restriction (presumably by assuming the same total volume of wax; see Botne 2012)
- Focus on how the information generated can be used to optimize pigging operations
- Obtain real composition for fields/pipelines suffering wax deposition.
- Effect of wall roughness (see Kjøraas 2013)

The assignment solution must be based on any standards and practical guidelines that already exist and are recommended. This should be done in close cooperation with supervisors and any other responsibilities involved in the assignment. In addition it has to be an active interaction between all parties.

Within three weeks after the date of the task handout, a pre-study report shall be prepared. The report shall cover the following:

- An analysis of the work task's content with specific emphasis of the areas where new knowledge has to be gained.
- A description of the work packages that shall be performed. This description shall lead to a clear definition of the scope and extent of the total task to be performed.
- A time schedule for the project. The plan shall comprise a Gantt diagram with specification of the individual work packages, their scheduled start and end dates and a specification of project milestones.

The pre-study report is a part of the total task reporting. It shall be included in the final report. Progress reports made during the project period shall also be included in the final report.

The report should be edited as a research report with a summary, table of contents, conclusion, list of reference, list of literature etc. The text should be clear and concise, and include the necessary references to figures, tables, and diagrams. It is also important that exact references are given to any external sources used in the text.

Equipment and software developed during the project is a part of the fulfilment of the task. Unless outside parties have exclusive property rights or the equipment is physically non-moveable, it should be handed in along with the final report. Suitable documentation for the correct use of such material is also required as part of the final report.

The candidate shall follow the work regulations at the company's plant. The candidate may not intervene in the production process in any way. All orders for specific intervention of this kind should be channelled through company's plant management.

The student must cover travel expenses, telecommunication, and copying unless otherwise agreed.

If the candidate encounters unforeseen difficulties in the work, and if these difficulties warrant a reformation of the task, these problems should immediately be addressed to the Department.

The assignment text shall be enclosed and be placed immediately after the title page.

Deadline: 30 June 2014.

Two bound copies of the final report and one electronic (pdf-format) version are required according to the routines given in DAIM. Please see <http://www.ntnu.edu/ivt/master-s-thesis-regulations> regarding master thesis regulations and practical information, inclusive how to use DAIM.

Responsible at Department:

Olav Egeland

Responsible supervisor:

Jon Steinar Gudmundsson

E-mail: jon.steinar.gudmundsson@ntnu.no

Telephone: 73594952

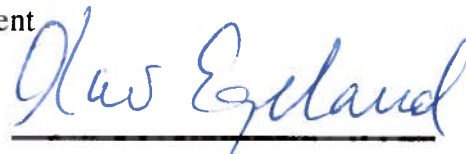
Supervisor(s) at Company:

**DEPARTMENT OF PRODUCTION
AND QUALITY ENGINEERING**



Per Schjølberg

Associate Professor/Head of Department



Olav Egeland

Abstract

Which criteria to pay attention to is important when finding the optimal pigging frequency. This thesis illustrates the forces acting on a bypass pig in operation. Expressions for both the frictional force and wax removal force have been presented. Results presented in this thesis show that the frictional forces are much higher than the forces for wax removal. The most important factor for the contact forces for a cleaning pig seems to be due to the oversize of the discs. However, it is difficult to obtain accurate values for the friction force without experimental data. The insulating effect of wax deposition on the overall heat transfer has been confirmed by analytical calculation. Results do also show that the simulation software Hysys do not account for wax deposition when estimation the U-value. Pressure drop calculations for a pipe with wax deposition have been done. Results show that the roughness of wax has a large influence on the pressure drop in a pipeline. Ageing of wax leads to higher wax removal forces and may decrease the removal efficiency for a cleaning pig. Pigging operations should happen at a given frequency to prevent wax from hardening. It would be beneficial to have more knowledge about wall adhesion and ageing for the given composition when estimation the wax removal forces.

Acknowledgments

The work presented in this master's thesis is a result of my master's degree in Subsea Technology. I would like to thank my advisor Jon Steinar Gudmundsson for his work with guiding me through this semester and for giving me the opportunity to work on this interesting topic. I would also like to thank Shuxin Hou for inputs and suggestions when forming the goals and content for the thesis, and for the help finding literature needed for the topic. I appreciate all the help, support and encouragement from my fellow students during my two years here at NTNU.

Table of Contents

Abstract	IX
Acknowledgments	XI
Nomenclature	XVII
1 Introduction.....	1
2 Heat Transfer.....	3
2.1 Heat Transfer Theory.....	3
2.2 Analytical Calculation of U-value for Pipe with Wax Deposition.....	6
2.3 Change in Overall Heat transfer Coefficient in Hysys	8
2.4 Change in Overall Heat transfer Coefficient with Wax Deposition in Hysys.....	10
2.5 Effect of Flow Velocity in a Pipeline with Hysys	11
3 Pigging Principles	13
3.1 Friction force	13
3.2 Forces for Removal of Wax Deposit	17
3.3 Bypass Flow through Pig.....	25
3.4 Pig effectiveness	28
4 Pressure Drop Calculations.....	29
4.1 Pressure Drop in Subsea Pipelines	29
4.2 Calculations with Focus on Wax Roughness	31
4.3 Calculations for Segmented Wax in Pipeline.....	34
4.4 Calculations for Slurry Flow	36
4.5 Calculations of Pressure Drop under Pigging Operation.....	37
5 Discussion	41
5.1 U-value Calculations	41
5.2 Pigging Principles.....	42
5.3 Pressure Drop Calculations	44
6 Conclusion	47

7	Further Work.....	49
8	References.....	51
	Tables	55
	Figures.....	59
	Appendices	i
	Appendix A – Calculation of friction for a pig	iii
	Appendix B – Derivation of formula for wax failure stress.....	v
	Appendix C - Derivation of formula for volumetric flow through an orifice	vii
	Appendix G - Calculation of the inside heat transfer coefficient h_i	ix
	Appendix H - Calculation of the outside heat transfer coefficient h_o	xi
	Appendix I.....	xiii

List of Tables

Table 1: Results from pressure drop calculations	35
Table 2: Pressure drop for slurry flow and clean pipe	37
Table 3: Pressure drop for slurry flow and wax deposition	37
Table 4: Properties for U-value calculations	55
Table 5: Thermal conductivity	55
Table 6: Fluid properties	55
Table 7: Assumed oil composition for the Norne field	56
Table 8: U-value results from simulations with Hysys	57
Table 9: Properties for pressure drop calculations	57
Table 10: Properties for pressure drop calculations with pig	58
Table 11: Properties for wax removal forces	58

List of Figures

Figure 1: Wax deposition vs. U-value. Analytical calculation.....	8
Figure 2: Simulation setup in Hysys	9
Figure 3: Temperature profile for a clean pipeline.....	9
Figure 4: U-value vs flow velocity.....	12
Figure 5: U-value vs Reynolds number (Logarithmic scale, base 10).....	12
Figure 6: Forces acting on a cleaning disc	15
Figure 7: Friction force vs pig velocity	17
Figure 8: Wax layer breaking force vs. porosity, Cup pig, wax thickness 4 mm	21
Figure 9: Wax removal forces for different oil contents in wax	22
Figure 10: Two possible models for wax removal	24
Figure 11: Typical force vs. distance behaviour	25
Figure 12: Wax removal with bypass pig	26
Figure 13: Viscosity vs. temperature for Norne oil composition.....	30

Figure 14: Oil density vs. temperature for Norne oil composition	31
Figure 15: Pressure gradient for different values for roughness in a pipeline with wax deposition	32
Figure 16: Calculated pressure drop for a clean pipe, with wax deposition and a Hysys simulation with wax	33
Figure 17: Pressure gradient for different wax distribution	35
Figure 18: Pressure drop for different wax distributions	36
Figure 19: Pressure drop in the pipeline including pressure drop across pig.....	38
Figure 20: Pressure profile with pig half way in pipeline	39
Figure 21: Norne composition	59
Figure 22: Inputs in Hysys for heat transfer coefficient estimation.....	59
Figure 23: Wax deposition profile for Hysys U-value estimation	60
Figure 24: Wax deposition profile for pressure drop calculations	60
Figure 25: Load vs. extension graph for various oil content wax samples	61
Figure 26: Wax deposit thickness vs. U	61
Figure 27: Pig velocity	62
Figure 28: Pressure drop increase for non-evenly distributed deposits	62
Figure 29: Friction and wax removal forces vs pipe length.....	63
Figure 30: Load model for wax removal	v

Nomenclature

Symbol	Description	Unit
A_{pig}	Area of pig that is affected by pressure	m^2
A_{pipe}	Inner pipe cross-sectional area	m^2
A_{pw}	Cross-sectional area of pipe with wax deposition	m^2
A_{wax}	Wax layer cross-sectional area	m^2
C	Wax breaking force coefficient	[-]
C_d	Discharge coefficient	[-]
C_p	Specific heat capacity	J/K·kg
D	Sample diameter	m
d	Pipe diameter	m
E	Young's modulus	N/m
F	Force	N
F_f	Friction force	N
F_{wax}	Wax removal force	N
g	Gravitational force	m/s^2
h_i	Inside heat transfer coefficient	$W/m^2 \cdot K$
h_n	Heat transfer coefficient for layer n	$W/m^2 \cdot K$
h_o	Outside heat transfer coefficient	$W/m^2 \cdot K$
ID	Pipe inner diameter	m
k	Thermal conductivity	$W/m \cdot K$

k_f	Thermal conductivity of the flowing fluid	W/m·K
k_n	Thermal conductivity of layer n	W/m·K
L	Sample length	m
l	Pipeline length	m
l_o	Original length	m
m_{pig}	Mass of pig	kg
N	Normal force	N
Nu	Nusselt number	[-]
OD	Pipe outer diameter	m
Pr	Prantl number	[-]
Q	Heat transferred	J
q_{oil}	Volume flow of oil	m^3/s
q_{wax}	Volume flow of wax	m^3/s
R	Thermal resistance	$m^2 \cdot K/W$
R_{fi}	Inside fouling thermal resistance	$m^2 \cdot K/W$
R_{fu}	Outside fouling thermal resistance	$m^2 \cdot K/W$
Re	Reynolds number	[-]
T	Temperature	°C
T_{in}	Temperature at pipe inlet	°C
T_2	Temperature at distance l in a pipeline	°C
T_u	Ambient seawater temperature	°C
T	Wax deposit thickness	m

U	Overall heat transfer coefficient	W/m ² ·K
u _{oil}	Oil flow velocity	m/s
u _{pig}	Pig velocity	m/s
w	Cleaning disc width	m
ΔT	Change in temperature	°C
ε	Extensional strain	[-]
η	Wax removal efficiency for pig	[-]
θ	Bypass area fraction	[-]
κ	Roughness value	mm
μ	Coefficient of friction	[-]
ρ _{oil}	Density oil	kg/m ³
ρ _w	Density sea water	kg/m ³
σ _d	Tension stress for a pig disc	Pa
σ _{wax}	Wax failure stress	Pa
τ _y	Yield stress	Pa
φ	Pig form factor	[-]
φ	Oil fraction in wax	[-]

1 Introduction

A vast amount of produced oil goes through subsea pipelines. A big part of this oil is located far away from shore, often in arctic areas and deep waters. This may cause flow assurance challenges such as paraffin wax, asphaltenes, hydrates, inorganic scale and sand accumulation. This master's thesis will only cover the wax problem.

The warm oil comes from the well and goes through the x-mas tree. When entering the subsea pipeline the oil starts to cool down due to ambient seawater temperature. As a result of this, the paraffin wax will start precipitate at a certain temperature. Further on, the wax may start to deposit on the pipeline wall. Precipitation and deposition can lead to major issues in forms of plugged pipes and production losses. The build-up of wax on the wall causes a reduced flow area and pressure drop in the pipeline. Unless the wax gets removed it will continue deposit in layers and even block the line. It is important to address the issues that may occur in a subsea pipeline. Paraffin wax also occurs in pipelines carrying condensate, that is, after processing on a platform. This is the case of the Heimdal-Brae pipeline.

The problem of wax deposition can be reduced by heating of the pipeline, inhibitors or by pigging. Pigging is the most common wax control method. The method allows wax to deposit on the wall and build up a wax layer before it gets scraped off. The frequency can vary from 2-3 days up to 3-4 months. It is important to find the right pigging frequency to reduce the costs and avoid flow problems. The oil companies often start with a high frequency to be sure to avoid stuck pigs in the pipeline, and reduce the frequency as they have gained more experience about the wax problem in the pipeline.

As the paraffin wax starts to deposit on the wall, the pipe cross sectional area will decrease. This decrease leads to pressure drop and flow restrictions, and can be an extensive challenge in the oil production.

As mentioned above the wax layer will build up in layers and can block the line if not removed. As the wax layer builds up, it becomes more difficult to pig the line. The forces needed to push the pig through the pipeline increases with increasing wax layer. With decreased pressure and flow in the line, and a large wax layer, there is a risk of the pig to get stuck. The wax thickness must be known to evaluate the likelihood of stuck pig.

The aim of this thesis is to investigate the forces acting on a pig in motion. The forces due to friction and wax removal will be discussed. This master thesis will take a look upon the topic and show results for calculations of the relevant forces. It is of interests to investigate which criteria to pay attention to when finding the optimal pigging frequency. Often earlier, only the thickness of the wax deposition has decided when to send a pig through the pipeline. The initial description of the thesis has been changed in co-operation with the supervisor, as the work has been evolved.

The effect of wax deposition in the pipeline with a focus on the total heat transfer coefficient will be evaluated in this thesis. As the wax layer increases, the total heat transfer coefficient changes/reduces and this affects the further wax deposition. The simulation software Hysys will be used to find a realistic wax deposition profile. Hysys will be tested to find out if the software account for the simulated wax deposition when estimating heat transfer coefficient. In addition, the oil flow velocity has an effect on the heat transfer. This effect will be explored and results for a subsea pipeline will be presented. A test will be conducted to check if Hysys account for the flow velocity when estimating the heat transfer coefficient.

The thesis will also include a chapter that addresses the pressure drop of a pipeline suffering wax deposition. As the wax layer is deposit on the wall the pipe diameter decrease, and the roughness increases. The pressure drop will be calculated for different wax distributions in the pipeline, and the results will be compared to the work done by Botne (2012). The thesis is limited to single phase liquid flow only.

2 Heat Transfer

2.1 Heat Transfer Theory

For subsea pipelines suffering wax deposition it is important to know the temperature profile. Knowledge about the heat transfer of the pipeline is essential when issuing the problem with wax deposition and when planning operational procedures. Oil flowing from a reservoir starts with a high temperature and it cools down during the transportation through subsea pipelines. The heat transfers from the oil, to the pipe steel and into the surrounding seawater. Normally a pipeline either rests on the sea floor, or is buried in the soil. The pipeline is surrounded by cold seawater at a constant temperature. The temperature at a given point in a pipeline can be calculated if the inlet temperature is known using Equation 2.3. Cooling of the fluid in the pipeline can with steady state flow be expressed as in Equation 2.1 and Equation 2.2.

$$Q = mC_p(T_i - T_u) \quad (2.1)$$

$$Q = UA(T_i - T_u) \quad (2.2)$$

$$T_{out} = T_u + (T_{in} - T_u) \exp \left[\frac{-U\pi d}{mC_p} L \right] \quad (2.3)$$

When calculating the temperature, the main uncertainty concerns the overall heat transfer coefficient (U). Because of this, it is of interest to see how the wax deposition affects the U-value for a pipeline. The heat transfer from oil to the surrounding seawater is dependent on the different layers of the pipeline. For subsea pipes the U-value for an uninsulated pipeline can be between 15 and 25 W/m²·K, and for an insulated pipeline the value can be as low as 1-2 W/m²·K. From this, the temperature of oil flowing in a pipeline will drop quickly for an uninsulated pipe. For an insulated pipeline the temperature decrease will be lower. The overall heat transfer coefficient U is the inverse of the thermal resistance R, see Equation 2.4 (Gudmundsson, 2009).

$$R = R_1 + R_2 + \dots + R_n \quad (2.4)$$

In nature three heat transfer modes occur, and heat is transferred by any one or combination of these three modes. The three modes are conduction, convection and radiation. Conduction

happens through a solid or a stationary fluid, convection from a surface to a moving fluid and radiation from all surfaces. For a subsea pipeline the radiation part is neglected because of the relatively low temperature of subsea system. For subsea pipelines conduction occur through the pipe wall and coatings, and to surrounding soil for buried pipelines. Convection occurs from the flowing oil to the pipe wall and from the outer surface of the pipe to the surrounding seawater (Bai & Bai, 2005).

The total thermal resistance can be written as Equation 2.4 when heat goes through many parallel layers. The total heat transfer can be written as Equation 2.5. As more resistance is added in form of a wax layer, the value of the heat transfer coefficient should decrease (Gudmundsson, 2009). The total heat transfer coefficient for a subsea pipeline can be calculated by using Equation 2.6 (Christiansen, 2011).

$$\frac{1}{U} = \frac{1}{h_1} + \frac{1}{h_2} + \dots + \frac{1}{h_n} \quad (2.5)$$

$$U_i = \left\{ ID \sum \left(\frac{\ln \left(\frac{ID_{n+1}}{ID_n} \right)}{2k_n} \right) + \frac{1}{h_i} + R_{fi} + \left(R_{fu} + \frac{1}{h_o} \right) \left(\frac{ID}{OD} \right) \right\}^{-1} \quad (2.6)$$

The Churchill-Berstein equation (2.6) is shown above. This formula can be used to calculate the U-value for an unburied subsea pipeline. For the formula above, k_n is the thermal conductivity for layer n. Subsea pipelines often consist of different insulation layers, and uninsulated pipes are normally made of steel with a concrete layer. Steel and concrete have very different thermal conductivity, and this needs to be given when calculating the overall heat transfer coefficient. In Equation 2.6 the inside heat transfer coefficient from the bulk fluid to the pipe wall is written as h_i . This is the heat coefficient in the laminar sub layer of the flow inside the pipeline. It is difficult to describe and semi-empirical correlations are used to calculate the coefficient. The inner heat transfer coefficient can be found with Equation 2.7. See Appendix G for an example of calculation of h_i . If steady state is assumed the Nusselt number can be expressed as a function dependent on Reynolds number and Prantl number, as in Equation 2.8, where n is 0.4 if the fluid is being heated and 0.3 when cooled (Bai & Bai, 2005).

$$Nu = \frac{hd}{k} \quad (2.7)$$

$$Nu = 0.0255Re^{0.8}Pr^n \quad (2.8)$$

The Reynolds number is a dimensional less number for expression the ratio of inertia to forces for viscous liquids. The Prantl number is a dimensionless number for expression the thermal properties of the bulk fluid. The equation for Reynolds number and Prantl number is 2.9 and 2.10 respectively.

$$Re = \frac{\rho ud}{\mu} \quad (2.9)$$

$$Pr = \frac{C_p \mu}{k} \quad (2.10)$$

Heat transfer from internal convection occurs between internal flowing liquid and the pipe wall. It depends on the pipe diameter, flow velocity and fluid properties. When the temperature of the flowing oil in the pipeline decreases, the fluid properties changes. The density, viscosity and heat capacity changes when the oil gets cooled. The relative large decrease in oil bulk temperature results in a small decrease in the overall heat transfer coefficient. This small decrease is not significant and does not affect the deposition of wax in the pipeline very much. When the fluid velocity increases the Reynolds number and Nusselt number increases. This gives in a higher inside heat transfer coefficient leading to a higher U-value from Equation 2.6.

The overall heat transfer coefficient does also depend on the outside heat transfer coefficient. As the cold seawater flows over the pipeline the steel will be cooled down. The outside heat transfer coefficient is written as h_o . An often used value for the sea current velocity is 0.1 m/s when calculation h_o . See Appendix H for an example of calculation of h_o .

The exposure of seawater depends on whether or not the pipeline is buried. When the pipe is partly or fully buried the mud or soil will have an insulating effect and the U-value will decrease because of this. Then the thermal conductivity of the actual soil needs to be known. Mud is often covering the pipeline. The mud is water saturated and acts as an insulator. In

Equation 2.6 this factor is written as R_{fu} and is called the outside fouling resistance. The formula for calculating the heat transfer resistance for the different layers of a pipeline is shown below (Christiansen, 2011).

$$R_n = ID \left(\frac{\ln \left(\frac{ID_{n+1}}{ID_n} \right)}{2k_n} \right) \quad (2.11)$$

When wax deposits on the pipe wall, it acts as an insulating layer due to low conductivity. The overall heat transfer coefficient depends on factors like pipeline conductivity, ambient and fluid temperature, and inner and outer heat transfer coefficient. If these parameters are held constant, the overall heat transfer will be held almost constant through the pipe. The wax layer deposits in a part of the pipeline, and changes the U-value locally for this area (Seyfaee, et al., 2012).

The change in overall heat transfer coefficient for a subsea pipeline affects the wax deposition. Results presented by Galta (2013) shows that the wax starts to deposit further into the pipeline for an increasing U-value. This affects the position of the peak value of the wax thickness (Galta, 2013). The wax layer gets thicker with time and when the temperature driving force for wax deposition decreases, the precipitated wax crystals will deposit further down the pipeline where the temperature difference is larger (Christiansen, 2011). The effect of insulation of a pipeline was tested in 2012 with Olga simulator. From this test, it was stated that the increase on insulation layer leads to a decrease in wax deposition. (Seyfaee, et al., 2012).

2.2 Analytical Calculation of U-value for Pipe with Wax Deposition

Analytical calculations have been done using Excel to see how large impact the wax deposition has on the overall heat transfer coefficient. To get a realistic value for the heat transfer coefficient the Churchill-Berstein equation is used, see Equation 2.6. The values used in calculation, such as thermal conductivity, heat capacity and viscosity for the flowing fluid is taken from Hysys with the given oil composition.

For the calculations a subsea pipeline surrounded by seawater with a temperature of 5 C is assumed. The pipe is made of carbon steel and has an outside layer of concrete. Inside the

pipe, a wax layer has been added. For the outside, a mud layer is accounted for as the outside fouling resistance. Values for the thickness of each layer of the pipeline, and the thermal conductivity values are taken from Christiansen, 2011. Table 4 shows the properties for the pipeline and the thickness of the different layers. Table 5 contains the thermal conductivities for the different materials, and Table 6 presents fluid properties.

Details such as reinforcement of steel in the concrete layer have been neglected. For a real subsea pipeline this may increase the U-value. Usually the subsea pipelines are resting on the seabed, or are partly or fully buried. Seabed soil can be a good insulator and do change the overall heat transfer coefficient. In present calculations a subsea pipeline without burial is assumed, and the surrounding sea current is acting on the whole outside area of the pipeline. The sea current velocity is set to 0.1 m/s, as is the default setup in Hysys.

The calculation of the inside heat transfer coefficient h_i and outer heat transfer coefficient h_o is shown in appendix G and H. First, a calculation for the U-value has been done with wax thickness from 0 to 10 mm. These results give numbers for the U-value that are close to the numbers given by Gudmundsson in 2009. He states that a common heat transfer coefficient for uninsulated pipelines is between 15-25 W/m²·K (Gudmundsson, 2009).

Secondly, a similar calculation has been done, but without the thermal resistance for the mud layer on the pipeline. In Hysys, the resistance from outer fouling is not accounted for when calculating the overall heat transfer coefficient. Because of this, similar calculation has been done in Excel to be able to compare the results. For estimation without the resistance from mud, the numbers for the U-value is larger than for calculations with the resistance. In addition, since the resistance from outer fouling is not present, other factor has larger impact on the overall heat transfer coefficient. Because of this, the drop in U-value due to wax deposition will be slightly larger for the second simulation. The same statement is included in the conclusion by Christiansen, 2011. The graph in Figure 1 shows the results for both the calculations.

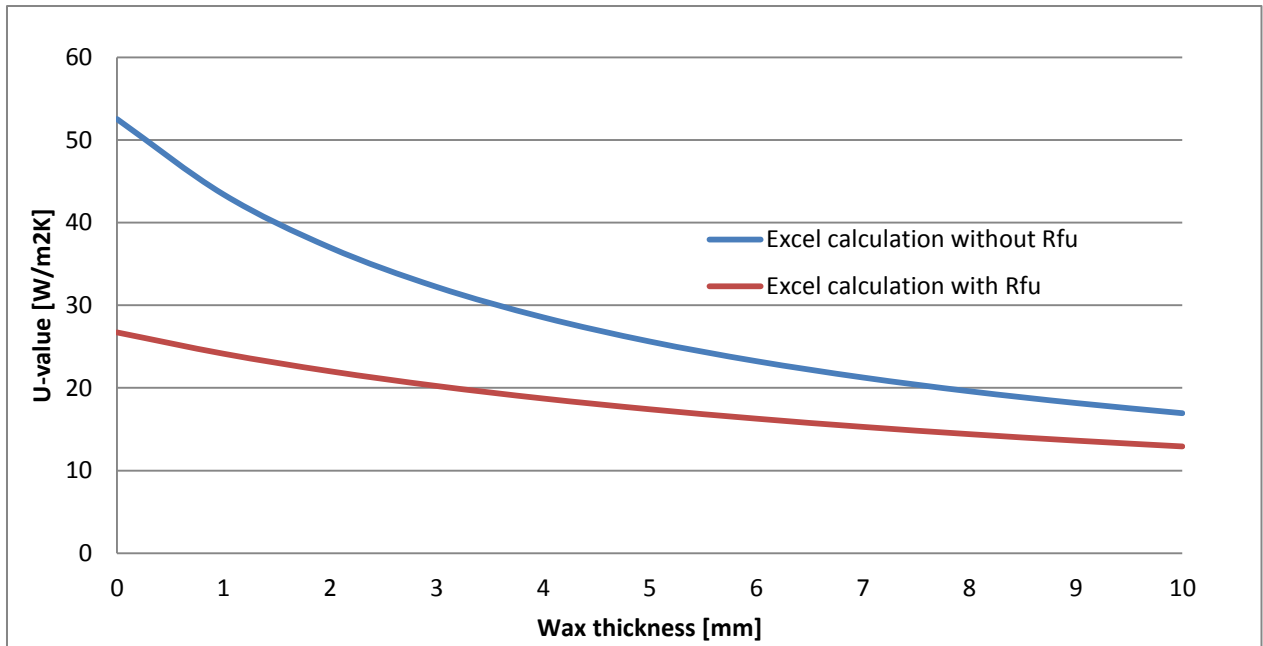


Figure 1: Wax deposition vs. U-value. Analytical calculation

2.3 Change in Overall Heat transfer Coefficient in Hysys

It is of interest to compare the results from the analytical calculations with numbers from Hysys. In Hysys it is possible to estimate an overall heat transfer coefficient for a pipeline. A test is done to check whether or not Hysys do account for the insulating effect of wax deposition when calculating the overall heat transfer coefficient. The software used is Aspen Hysys V.8.3.

To test the effect of wax in the pipeline with Hysys, a reference simulation has been done. This simulation was done without wax deposition to see how Hysys calculated the overall heat transfer coefficient. In order to perform the tests, the pipeline in the program was divided into segments. This allows the U-value to be calculated in different parts of the pipe, instead of a general number for the whole pipeline. A 12000 meter long pipeline is divided into 12 segments to check the U-value of each part of it. Figure 22 shows the inputs in Hysys for the heat transfer coefficient estimation. An oil composition from Norne is used. The composition is presented by Galta (2013) and can be found in Figure 21 and Table 7. The inlet temperature for the oil is set to 45 C, and the flow velocity used for the simulation is 1 m/s. This flow

velocity equals volume rate of approximately 255 m³/h. Figure 2 shows the setup used for the simulation. The temperature profile for the simulation can be seen in Figure 3.

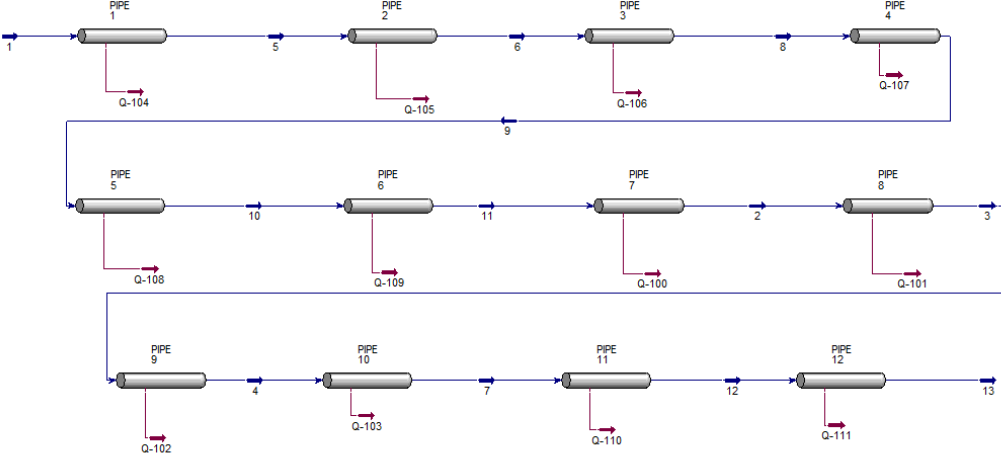


Figure 2: Simulation setup in Hysys

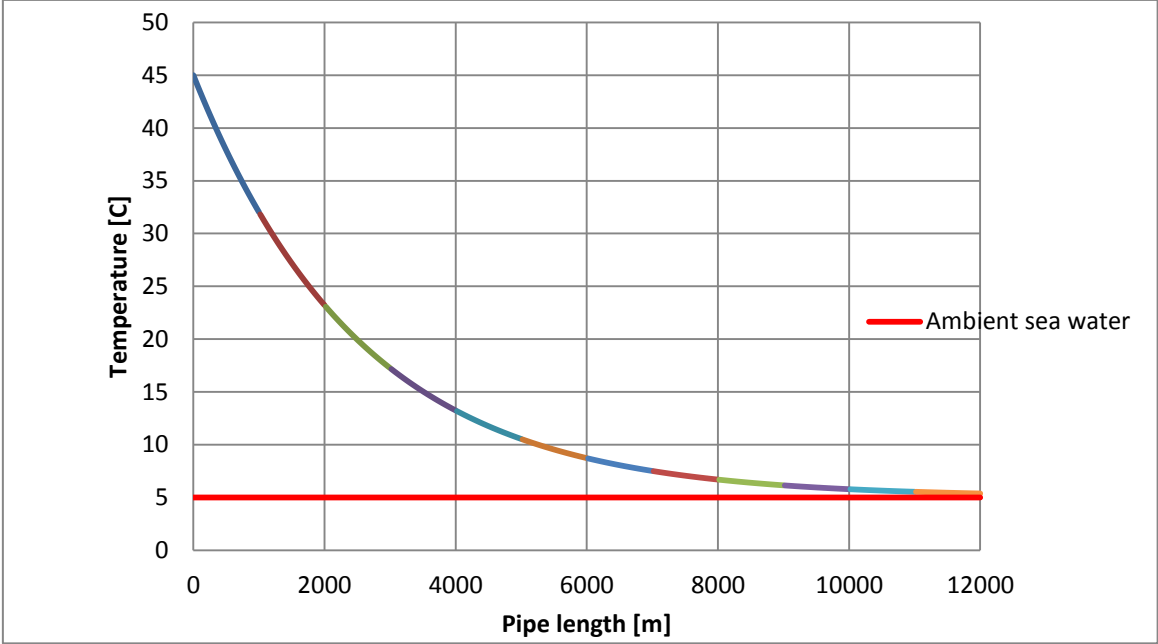


Figure 3: Temperature profile for a clean pipeline

Hysys presents the U-value for the pipeline based on the outer diameter. Usually, pipeline designers use a U-value based on the inner diameter, while insulation manufacturers use a value based on the outer diameter. The relationship between the U-value for outer and inner

diameter can be seen from equation 2.12. U_o is U-value for the outer diameter, while U_i is for the inner (Bai & Bai, 2005).

$$U_o OD = U_i ID \quad (2.12)$$

The results from the reference simulation in Hysys are listed in Table 8. The overall heat transfer coefficient is from the results decreasing for each segment. This small change in the U-value is assumed to be due to the temperature change.

2.4 Change in Overall Heat transfer Coefficient with Wax Deposition in Hysys

A second simulation was done with Hysys to check the estimated overall heat transfer coefficient for the pipeline. The same properties as given above were used in this simulation. However, this time a simulation of wax deposit were added. A description for how to simulate the wax profile was given by Galta (2013). The wax deposit is simulated for 7 days and Figure 23 shows the profile of wax deposition for the pipeline.

The thermal conductivity of wax is 0.25 W/m·K and it is expected that the wax deposit will act as an insulation layer (Christiansen, 2011). If Hysys is taking into account the insulating effect, the total U-value must change for each of the segments when the pipe has wax deposition along the profile. The calculated value for the subsea pipeline without wax deposition ranged from approximately 58 W/m²·K at the inlet to 55.7 W/m²·K at the outlet. The results from analytical calculations in Chapter 2.2 show that the U-value has been reduced by 10 W/m²·K for 1 mm wax layer. For a 2 mm wax layer the U-value is further reduced with 6 W/m²·K. For this reason the estimation of U-value with wax deposition should give lower values than in Chapter 2.3.

The results from Hysys for estimation of the overall heat transfer coefficient with wax deposition gives the same results as in Chapter 2.3. Hysys estimates the same U-value with and without simulated wax deposition in the pipeline. This means that Hysys do not account for simulated wax deposition when calculating the overall heat transfer coefficient.

In addition to simulate wax in the pipeline as a function of the time, it is also possible to insert an initial layer of wax in the pipeline. This gives the opportunity to estimate the U-value of the pipeline with an evenly distributed layer of wax. A third simulation was done. This time a

2 mm evenly layer of wax deposit was applied to the pipeline. Once again, Hysys estimated the same results as in Table 8.

The results from this chapter show that Hysys does not account for the insulating effect of wax deposition. The small drop in U-value is due to the temperature change of the flowing oil. The graphs from analytical calculations show that the wax deposition changes the overall heat transfer coefficient.

The results between the analytical calculations, and the numbers estimated by Hysys for a clean pipe corresponds well. Hysys estimated an overall heat transfer coefficient of 57.9 for the first segment, while the calculation from Excel gives a value of 55.1. This gives a deviation of 5%.

2.5 Effect of Flow Velocity in a Pipeline with Hysys

It was stated by Galta (2013) that the velocity of the flowing fluid had an effect on the wax deposition in a subsea pipeline. To check whether or not Hysys uses the flow velocity when calculating the U-value, a test simulation is done. In order to complete this test all parameter has been constant except for the flow velocity. The simple setup consisting of an inlet flow, a pipe segment and an outlet flow in Hysys. In the test, a velocity range from 1-6 m/s is used. This is due to the recommended maximum flow velocity in regular carbon steel pipelines by Norsok (Norsok Standard, 2006). The results are shown below in Figure 4.

From the graph below, Hysys gives slightly higher values for the U-value, but the shape of the curve is similar. These results show that the overall heat transfer coefficient increases with increasing flow velocity. It also shows that the simulation software Hysys does account for the flow velocity when estimating the U-value. Figure 5 presents the U-value plotted against Reynolds number. Reynolds number increases with velocity, and the Nusselt number is dependent on the Reynolds number. See Equation 2.8 and 2.9.

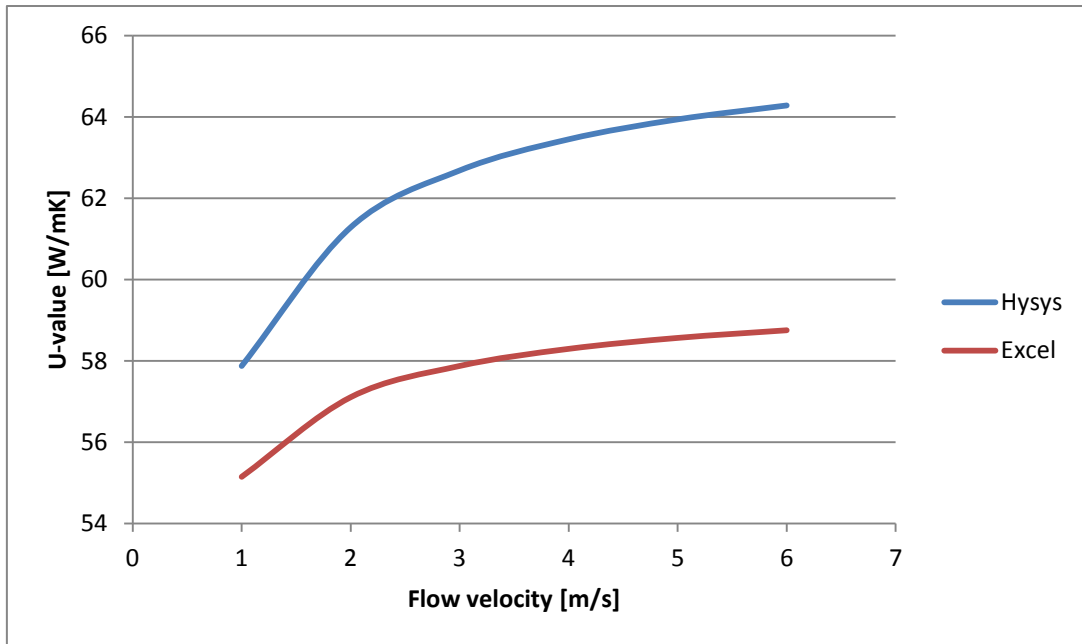


Figure 4: U-value vs flow velocity

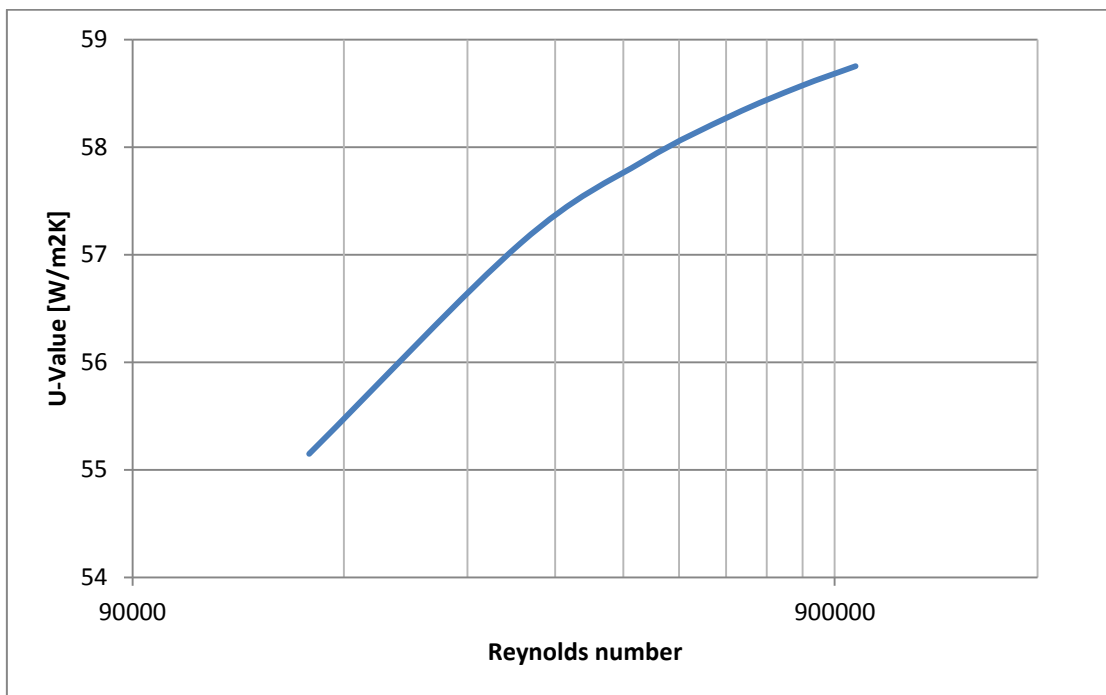


Figure 5: U-value vs Reynolds number (Logarithmic scale, base 10)

3 Pigging Principles

In this chapter the forces acting on a cleaning pig in operation will be investigated. The pig is driven forward by fluid pumped upstream of the pig. The fluid provides necessary pressure to overcome the forces for keeping the pig moving. This chapter is limited to mandrel cleaning pigs made from flat disc cups attached to a cylindrical body. Professor Gudmundsson has written a Technical Note that considers the forces required to remove wax deposits. The structure of this thesis is inspired and formed by this note. The paper is added to Appendix I.

The friction forces acting on the pig and the wax removal forces dictates the amount of differential forces needed to push the pig forward. The prediction of the forces acting on a pig in motion is a difficult task due to the complexity of geometries and different pigs. In present thesis simplifications are used to show which major forces to pay attention to, in addition to present quantitative numbers for the forces. The pressure force acting on pig can be described by Equation 3.1, where ΔP is the differential pressure across the pig, and A_{pig} is the area of the pig that is affected by the pressure.

$$F_{pig} = \Delta p A_{pig} \quad (3.1)$$

$$F_{pig} = (p_1 - p_2) \frac{\pi d^2}{4} \quad (3.2)$$

3.1 Friction force

The frictional force acting on a pig in motion can be divided into two parts. The first one is the well-known equation $F_f = N\mu$ where N is the normal force and μ is the coefficient of friction. N is the product of the factors m and g , where m is the mass of the pig (kg) and g is the gravitational force (m/s^2). In addition to this force there must be force acting on the whole outer area of the pig discs. The size of the scraping discs on a pig is from 102 % to 105 % of the inner pipe diameter (Davidson, 2002). This means that the discs must be compressed to fit into the pipe. According to Hook's Law a force will act in the opposite direction when the

disc is elastically compressed. The force acts on the outer area of the discs and the tension is found from Equation 3.3. By introducing the Young's modulus E , an expression for the tension can be found. Equation 3.4 gives the tension for the pig discs, where ϵ is the extensional strain due to compression.

$$\sigma_d = \frac{F}{A} \quad (3.3)$$

$$\sigma_d = \epsilon E \quad (3.4)$$

$$\epsilon = \frac{\Delta L}{L_o} \quad (3.5)$$

The Young's Modulus is a measure of stiffness for a material. The discs on a pig are usually made of polyurethane elastomer, and the Young's modulus differs. In an earlier paper 8 MPa and 13 MPa are used as the Young's modulus (Nieckele, et al., 2001). The contact forces due to compression of the pig discs are called post buckling by Nieckele, et al, (2001).

Simulations have been done by Nieckele, et al, (2001) for disc pigs with a Young's modulus of 13 MPa and 8 MPa. The results for a 1 m diameter pipe are around 30 kN up to 55 kN for the range 1 % - 7 % in oversize. When determining the contact forces it was already in 1996 observed that oversize of the pig discs is the most important factor (Azevedo, et al., 1996). Equation 3.6 and 3.7 gives the expression for friction forces acting on a pig in motion with post buckling:

$$F_f = N\mu + A_d n \sigma_d \mu \quad (3.6)$$

$$F_f = m_{pig} g \mu + 2\pi r w \sigma_d \mu n \quad (3.7)$$

Where m_{pig} is the mass of the pig (kg), g is the gravitational force (m/s^2), μ is the dimensionless coefficient of friction, A_d is the outer area of the scraping discs, w is the width of each disc (m) and n is the number of discs. If other resistive forces are ignored, the force balance for constant speed of the pig will be:

$$F_{pig} = F_f \quad (3.8)$$

$$\frac{\pi d^2}{4} \Delta P = \mu(N + A_d n \sigma_d) \quad (3.9)$$

Expressed for the differential pressure required to overcome the frictional forces:

$$\Delta P = \frac{\mu(N + A_d n \sigma_d)}{A_{pig}} \quad (3.10)$$

From this expression it is possible to alter the contact forces for a pig in operation. By lowering the oversize value of the sealing discs the forces will decrease. Also the seal disc width and the material hardness can be adjusted to increase or decrease the friction forces. For high friction pigging it is of desire to achieve higher friction forces. High friction pigging will not be further discussed in present thesis. Figure 6 show how the cleaning disc acts when pig is in motion and how the differential pressure acts on a curved disc.

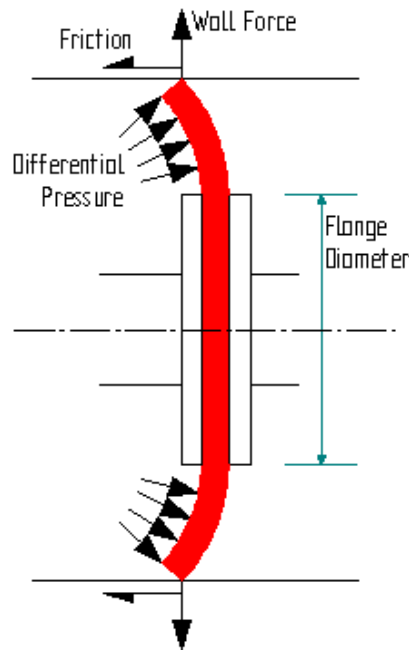


Figure 6: Forces acting on a cleaning disc (Pipeline-research.com, 2002)

The coefficient of friction is dependent on the material of the pig, the pipe wall and on lubrication. The pipe wall is made of steel and can have different surface roughness. Lubrication between the two materials has a major influence on the friction. In this case the

oil will function as lubrication between the surfaces and lowers the value for friction. In the case of wax removal, fractions of wax may still cover parts of the surface. If the wax is not completely removed, it will affect the friction. It is because of this difficult to obtain a realistic value for the situation, and an exact number needs to be measured by experiment. It was stated by Wu & Spronsen (2005) that the recommended value for the friction coefficient ranges between 0.02 and 0.05 in the paper about slug reduction in a gas pipeline (Wu & Spronsen, 2005). Data from Nieckele, et al, (2001) gives fairly good agreement between experimental and numerical results with a friction coefficient of 0.4 (Nieckele, et al., 2001). For the first term in Equation 3.7 the mass of the pig decreases in an oil filled pipeline. The mass changes with a buoyancy factor for the fluid. For a 50 kg pig in oil with density of 780 kg/m³, the mass will be 43 kg. For this calculation a relation of 2/3 for steel and 1/3 polyurethane is assumed for the construction of the pig. For lighter pigs like foam pigs and solid cast pigs, the weight is very low. The first term in Equation 3.7 then gives a very small value for the normal friction force. Despite this, the buoyancy effect is not a major factor for the calculation of the friction force.

For a pipe with inner diameter of 0.3 m and 103 % oversized discs the force per disc will be 2.7 kN. This is calculated using equation the second term in Equation 3.7. If the number of discs per pig is 6, the total friction force for a 50 kg pig is 16.5 kN. See Appendix A for calculation. The percent of oversize of the disc is a major factor for the contact force. For an oversize of 101 % the friction force is 5.6 kN, while it is 27.3 kN for 105 % oversize.

When the pig is in motion the frictional forces is high enough to make the discs buckle to fit into the pipe (Nieckele, et al., 2001). This may change the contact forces between the pig and pipe wall and the forces depends on the pig velocity and how much the discs is flipped.

Botros & Golshan (2010) present results from a test performed in Canada. They give the formula:

$$F_c = c_o + c_1 u_{pig} + C_2 u_{pig}^2 \quad (3.11)$$

Where $C_o = 150$ N, $c_1 = -4.0$ N.s/m and $c_2 = 0.04$ N.s²/m². u_{pig} is used as the pig velocity. This gives a polynomial friction curve. The friction between the pig and pipe wall is dependent on the pig velocity (Botros & Golshan, 2010). This gives 142 N in friction forces for a pig velocity of 2 m/s. This value is much lower than the one calculated above, and this equation is presented in a paper concerning gas pipelines with an intelligent pig used for inspection.

Figure 7 presents the frictional force from Equation 3.11 plotted against pig velocity. It is common to use a pig velocity between 1-5 m/s (Botros & Golshan, 2010).

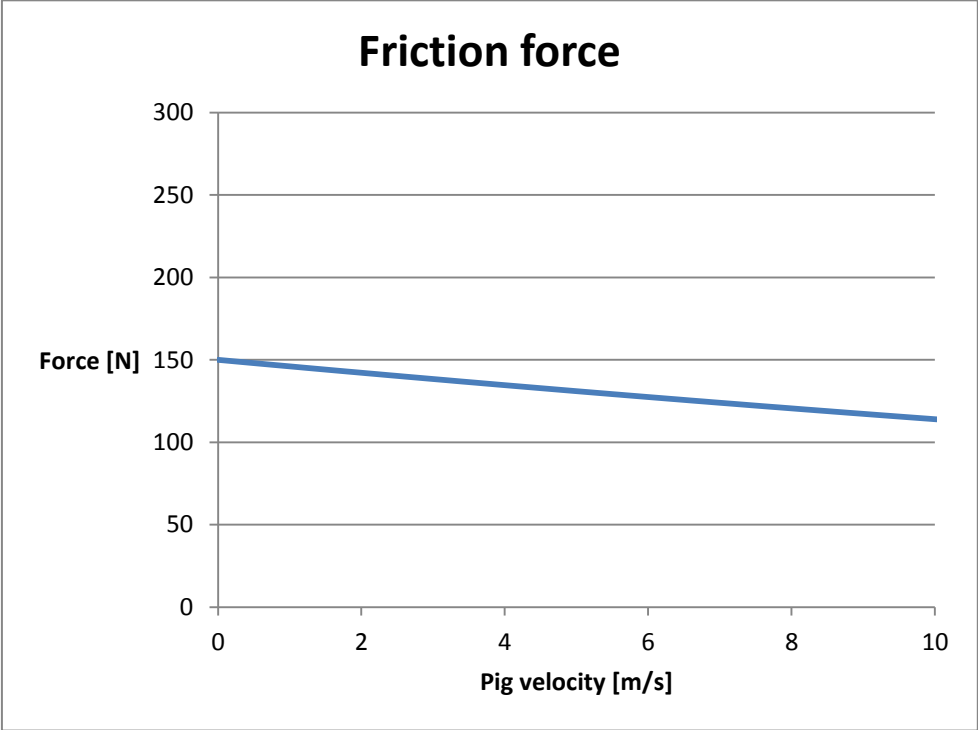


Figure 7: Friction force vs pig velocity

3.2 Forces for Removal of Wax Deposit

Experimental data shows that the force for removal of wax deposition can be the most important factor and, sometimes, the only responsible for pig stall (Barros, et al., 2005). It is therefore a very important factor when calculating the total forces acting on a pig. The wax removal forces needs to be elucidated in order to get realistic values for forces acting against the pig movement.

It can be assumed that a mechanical cleaning pig breaks loose the wax by applying a certain force in the axial direction on the cross section of the deposit. Then, the force for breaking the wax will be the area of wax in the pipe times the axial stress for loosening the wax. The wax removal force can be expresses as:

$$F_{wax} = \sigma_{wax}A_{wax} \quad (3.12)$$

A_{wax} is the cross-sectional area of the wax deposit. Equation 3.13 and 3.14 shows the derivation of the expression for the wax removal force. The thickness of wax is written as t , and d is the inner diameter of the pipe. σ_{wax} is the failure stress of the wax. This gives a very simplistic expression for the wax removal force.

$$A_{wax} = \frac{\pi d^2}{4} - \frac{\pi(d-t)^2}{4} = \pi(td - t^2) \quad (3.13)$$

$$F_{wax} = \sigma_{wax}(\pi(td - t^2)) \quad (3.14)$$

For calculation of the wax removal forces it is important to have a look at the physics of wax under removal. It is different ways of modelling how the wax is removed from the wall. Southgate (2004) has discussed this in his thesis about wax removal. He showed that in some cases the wax adheres so poorly to the pipe wall that the force needed to fracture the wax interface may be neglected. If the deposits do not adhere well to the wall the cohesive strength of the material is of low importance. It is suggested from field reports that the adhesive strength of wax deposit is at least equal to their cohesive strength. For situations with low adhesion the wax deposit will fail at the pipe wall and come off as flakes (Southgate, 2004).

The thesis by Southgate (2004) also gives an assumption that under real wax removal situations, the wax deposit fails at the pipe wall due to conditions enforced by the geometry of the scraping tool. Further a conclusion is drawn that the physical properties of paraffin wax deposits varies with the crude oil, thermal environment, ageing and flow regime. This makes it difficult to predict the physical structure and properties of wax deposit. Wax removal methods must therefore be aimed at deposits with a broad spectrum of properties (Southgate, 2004). How wax adheres to the pipe wall is an important factor to have knowledge about. If the adhesion force is strong, the thickness of the wax deposit is very important for the forces required to break the layer. If the wax adheres poorly to the pipe wall, the wax thickness may be of less importance if the wax is assumed to flake of the wall.

Southgate (2004) did also compare wax cutting to orthogonal metal cutting theory. It was discovered that for greater depths of cut, the process of wax cutting is less predictable than

metal cutting. When wax is cut, a mode of failure occurs that cannot be described by conventional metal cutting theory (Southgate, 2004).

Wax deposits consist of a mixture of wax and oil. The fraction of oil trapped in the wax deposit depends on the flow regime. Turbulent flow with higher shear stress at the wall may lead to wax deposit with lower oil percent. When wax deposits on the pipe wall it forms an interlocking crystal matrix that is trapping amounts of oil in the deposit (Zhang, et al., 2014). The amount can vary from 0 % to over 90 %. The amount of oil in wax deposit is calculated as the volumetric fraction of oil to the total deposit and is called the wax porosity. Higher amounts of oil in the mixture lead to a softer deposit. In the case of pigging, this means that a deposit layer with low porosity is harder to remove than a soft oil filled layer. Over time the oil content of the deposit diffuses out of the solid wax mixture. This is called ageing and makes the deposit harder with time. (Siljberg, 2012)

The wax deposition build-up will stagnate after a given time. Because of the ageing effect of wax, the pigging frequency still needs to be kept at a certain interval. Simulations will typically predict the wax deposit increase with time without considering the shear removal mechanism. The shear removal effect will always be present in a real field pipeline, and prevents continuous wax build-up with time. After a certain time the shear removal rate will be in balance with wax build up, and the wax thickness growth stops (Zhang, et al., 2014).

The oil molecules continuously diffuse out of the deposit, and in addition, wax molecules may diffuse into the wax deposit. This leads to an increased wax fraction and lower wax porosity. The wax ageing process can harden the wax deposit and make the wax removal more difficult. The effect of ageing of wax deposition was tested by Zhang, et al, (2014). A conclusion from these tests says that the ageing process does not have a significant effect on the growth of the wax deposition profile. However, the wax ageing leads to a lower wax porosity and increase the hardness of the deposit (Zhang, et al., 2014).

Several tests have been done on wax samples in a PhD thesis by Southgate (2004). To describe the failure stress for wax, Equation 3.15 is used. For the formula, F is the force in vertical plane, L is the length of the sample and D is the sample diameter.

$$\sigma_{wax} = \frac{2F}{\pi LD} \quad (3.15)$$

For pure wax samples the failure stress for a “Brazil” compression test was found to be 676 kPa, 596 kPa and 422 kPa. Southgate did also conduct a “Modulus of Rupture test (MOR)” to determine the flexural strength of the wax. The results from the “Brazil” and “MOR” tests give a mean average tensile strength of 1.3 MPa for the test samples. The Tresca yield criterion was introduced to describe the shear stress on the samples. This criterion is based on the assumption that yielding of a material occurs when the maximum shear stress reaches a critical value (Southgate, 2004). For this case, the critical shear stress is given by Equation 3.16. The mean average yield stress calculated from the Tresca criterion is 0.28 MPa, by using numbers from the “Brazil” test.

$$\tau_y = \frac{\sigma_{wax}}{2} \quad (3.16)$$

Further wax samples made of wax/oil mixtures were tested. Samples with 100 %, 75 %, 50 % and 25 % wax were included in the experiment. Figure 25 shows the results. It can be seen from the graph that pure wax samples behave in a brittle manner and goes to failure. Samples with oil become more ductile and it requires less force before it begins to flow. Southgate (2004) reports that there is no tensile failure for wax mixture with 50 % oil content or more, and it acts more like a “Bingham” fluid. Because of the more ductile behaviour of the wax, Equation 3.15 does not describe the stress state at failure for the 50 % wax mixture (Southgate, 2004).

$$F_{wax} = C\tau_y(\phi)t\pi d\eta(1 - \varphi) \quad (3.17)$$

Equation 3.17 for wax removal force is presented in a paper by Hovden, et al, (2004). For the formula C is a breaking force coefficient, $\tau_y(\phi)$ is the yield stress of the wax as a function of the oil/condensate fraction, and η is the efficiency of the wax removal. The breaking force coefficient is used for the effective shear surface orientation. A coefficient value of 1 implies that the shear surface is normal to the pipe wall. For an effective shear surface of 45°, the coefficient value will be $\sqrt{2}$ (Olga, 2011). When the maximum failure stress is applied to the wax deposit a shearing effect occurs and the wax breaks. Southgate (2004) states to have observed a shear angle of 45° in his experiments. A coefficient value of $\sqrt{2}$ can be assumed in calculations. In the formula, φ is the pig form factor.

The pig form factor is a measure of the efficiency of the cutting of wax. A sharp cutting device will have a factor value close to 1. For a disc pig, foam or cup pig the form factor will be closer to zero (Hovden, et al., 2004). A different geometry of the cutting tool (the pig disc) could help to lower the wax removal force.

The expression $\tau_y(\phi)$ is presented as Equation 3.18 in the paper by Hovden, et al, (2004) for a wax sample with given properties. Equation 3.19 presents a more general expression for the yield stress of wax deposit. With this formula the wax removal force F_{wax} depends linearly with the oil/condensate content of the wax deposit. In the equation, τ_y is the yield stress for a 100 % wax sample. As the porosity of the wax increases, more oil is filled in the deposit. This makes the deposit weaker and forces needed to remove the wax decreases. Figure 8 from Hovden, et al, (2004) shows the breaking force vs. the wax porosity. The breaking force is calculated using Equation 3.17. As seen in the figure, the breaking force starts to increase even more when the porosity goes below 50 %. This gives a good correlation with the experiments done by Southgate (2004).

$$\tau_y(\phi) = 1.25 \cdot 10^6 \cdot (1 - \phi)^4 \tag{3.18}$$

$$\tau_y(\phi) = \tau_y \cdot (1 - \phi) \tag{3.19}$$

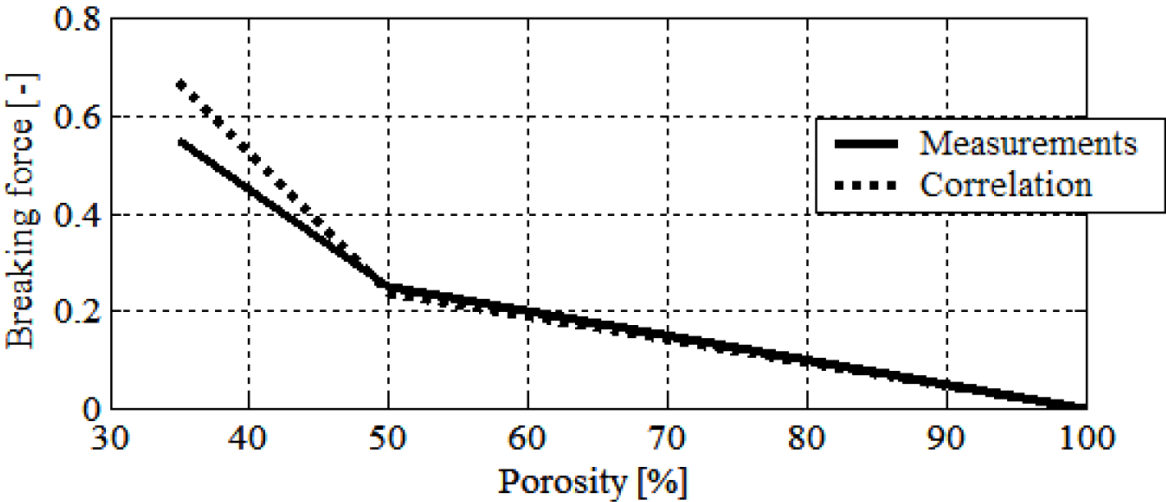


Figure 8: Wax layer breaking force vs. porosity, Cup pig, wax thickness 4 mm (Hovden, et al., 2004)

Numbers taken from Table 11 is used to calculate the wax removal forces for a pipeline with wax deposition profile. The profile used can be seen in Figure 24. The result is shown in Figure 9. For the maximum wax thickness of roughly 3.6 mm and an oil/condensate fraction of 30 % the calculation will be as below. Equation 3.17 is used for the calculation. Equation 3.19 is used to adjust for oil content, since the wax failure stress is found from a pure wax sample.

$$\tau_y(\phi) = 0.28 \cdot 10^6 \cdot (1 - 0.3) = 196\,000 \text{ Pa}$$

$$F_{wax} = \sqrt{2} \cdot 196\,000 \text{ Pa} \cdot 3.6 \cdot 0.001 \text{ m} \cdot \pi \cdot 0.3 \cdot 0.95(1 - 0)$$

$$F_{wax} = 893 \text{ N}$$

Compared to the frictional forces between the pig and the pipe, this force is rather low. Figure 29 shows both the friction force and wax removal force. The influence of wax removal is not very large for the total resistive force.

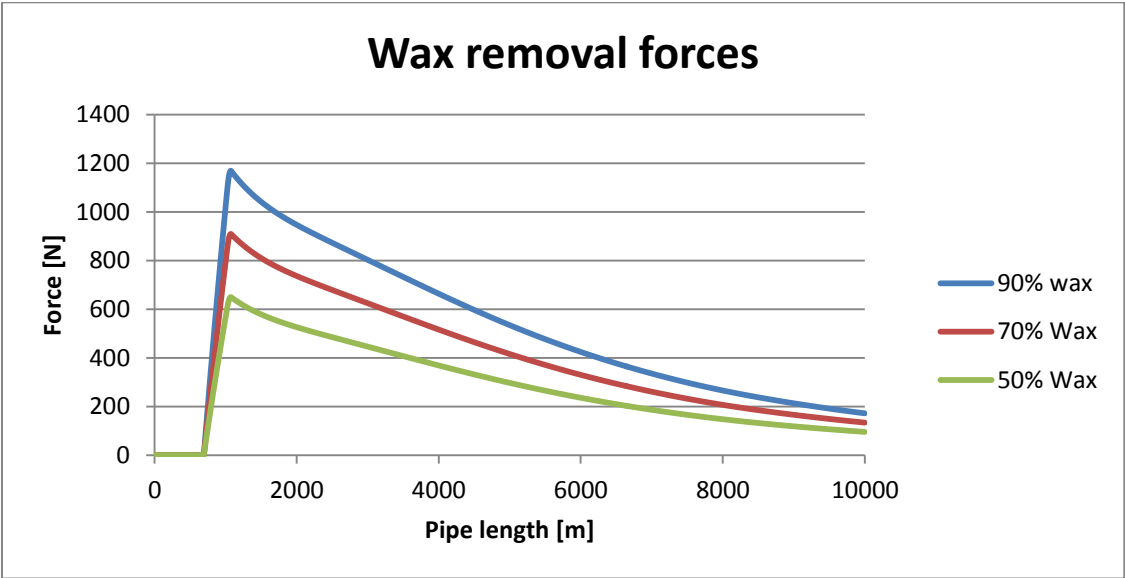


Figure 9: Wax removal forces for different oil contents in wax

Two load models for wax removal were evaluated by Mendes, et al, (1999). The models are shown in Figure 10. The first model is for more rigid cleaning pigs and implies breaking of the wax, as assumed in Equation 3.12 and 3.17. The equation for the first load is presented by Mendes, et al, (1999) as:

$$\sigma_{wax} = \frac{\Delta P}{\left(\frac{4t}{d}\right) \left(1 - \frac{t}{d}\right)} \quad (3.20)$$

For this model the pig acts axially on the deposit and the wax will be removed by applying shear stress. ΔP is the differential pressure needed across the pig to overcome the mechanical shear resistance of the wax. This equation gives the same value for the wax failure stress as for an equation presented by Southgate (2004). See Appendix B for derivation. This equation can be used to calculate the pressure differential across the pig needed to remove a given wax thickness.

While load model 1 implies breaking of the wax layer, the pig only scrapes the surface of the wax in load model 2. The second model is based on deformable pigs, like foam pigs. They are softer and more likely to ride over the wax layer and impose a shear stress on it. It was observed in experiments by Barros, et al, (2005) that the efficiency was poorly for the foam pigs acting in the way of load model 2. In all the cases the wax removal was not completed in the experiment. To comparison, all the pigs implying load model 1 had 100 % wax removal efficiency (Barros, et al., 2005). The shear stress imposed on the wax layer by a pig for load model 2 is:

$$\tau = \left(\frac{\left(\frac{1}{2} - \frac{t}{d}\right)}{2 \cdot \frac{L}{d}} \right) \Delta P \quad (3.21)$$

The parameter L/d is the dimensionless axial length of contact between the pig and the wax layer (Mendes, et al., 1999). The normal load on the wax deposition from the pig is given as in Equation 3.22. Explanation of the load models in shown in Figure 10.

$$\sigma = \frac{1}{\mu} \cdot \left(\frac{\frac{1}{2} - \frac{t}{d}}{2 \cdot \frac{L}{d}} \right) \Delta P \quad (3.22)$$

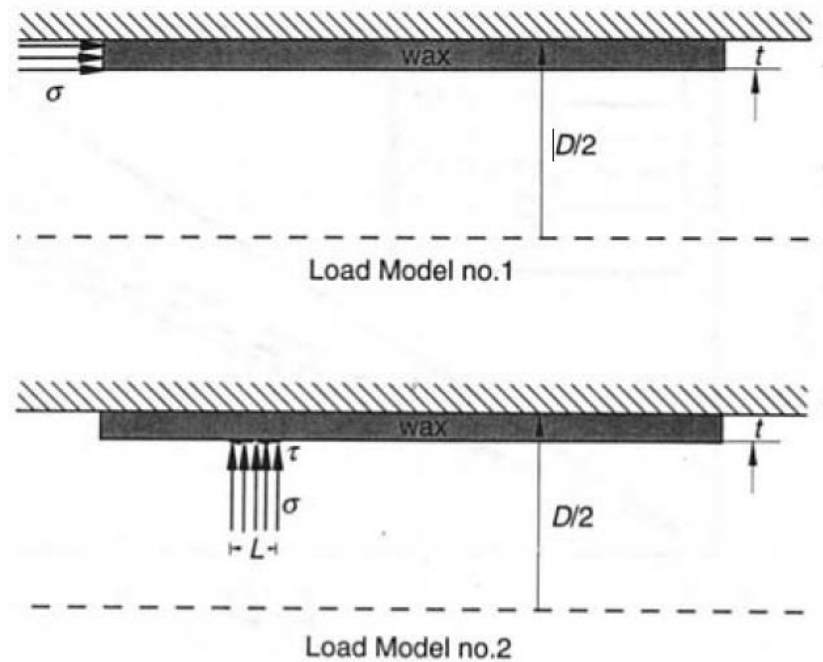
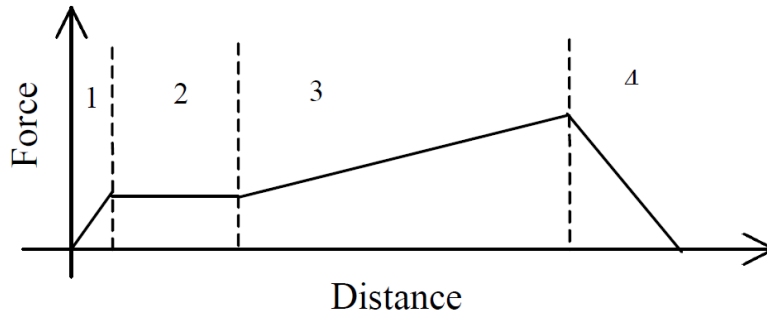


Figure 10: Two possible models for wax removal (Mendes, et al., 1999). Modified by (Barros, et al., 2005).

Experiments for finding the forces for wax removal were done by Barros, et al, (2005). Different types of pigs were tested, giving different results. For a disc pig in a pipe with inner diameter of 75 mm and a 3 mm wax layer, the removal force was found to be 530N (Barros, et al., 2005). By using Equation 3.12 the strength of wax can be calculated to 721 kPa. The compressive strength of paraffin wax is by experiments found to be 658.4 kPa by (Hossain, et al., 2009). This is for a sample of 100 % wax. In the experiment by Barros, et al, (2005), the efficiency of the disc pig was found to be 100 % and the wax was removed in a manner consistent with load model 1.

Wang, et al, (2005) identified four distinct phases of the wax removal forces. After the breakage of wax deposit it accumulates and forms a plug downstream of the pig (Wang, et al., 2005). The same behaviour was seen in the experiments done by Barros, et al, (2005). The forces for wax removal were observed to increase up to three times the value originally required to break the deposits. The dislodge wax gets compressed in front of the pig creating a plug. The forces acting against the motion increases until the available pressure level upstream of the pig is no longer sufficient to drive the pig and the wax plug. The development for the forces because of wax accumulation in front of pig is shown in Figure 11. This observation is corroborated with field information and seems to be the reason for pig stalling in several situations (Rønningsen, 2012). By introducing the bypass flow for a pig this problem can be avoided. The removed wax particles get flushed away by the bypass flow and

the only resistive forces applied by the wax layer are the forces needed to break the wax from the pipe wall. The equations for the opposing forces in present thesis assume no wax accumulation.



- | | |
|-------------------|----------------------|
| 1 – Buildup phase | 2 – Pre-plug phase |
| 3 – Plug phase | 4 – Production phase |

Figure 11: Typical force vs. distance behaviour (Wang, et al., 2005).

3.3 Bypass Flow through Pig

Bypass flow through the pig is introduced to prevent wax accumulation downstream of the pig. As mentioned in Chapter 3.2, the dislodge wax in front of the pig gets compressed and forms a solid plug. The plug formation leads to increasing frictional forces between the wax plug and the pipe wall. Bypass allows the driving oil to flow through the mandrel or through holes in the scraping discs. The volumetric flow through the orifice of the pig can be found by an expression derived from Bernoulli’s equation. See Appendix C for derivation of equation 3.23.

$$q_{bp} = C_d \sqrt{\frac{2\Delta P}{\rho_{oil}}} A_{bp} \quad (3.23)$$

The differential pressure across the pig needs to be large enough to overcome the resistive forces acting on the pig. For equilibrium, the pressure force acting on the pig must equal the resistive forces F_{wax} and F_f .

$$F_{pig} = F_f + F_{Wax} \quad (3.24)$$

The opposing forces F_f and F_{wax} is calculated above respectively in Chapter 4.1 and 4.2. The force required to push the pig is:

$$F_{pig} = 0.9kN + 16.5k = 17.4kN$$

The pressure differential across the pig required to overcome the forces is from Equation 3.1 as follows:

$$\Delta P_{pig} = \frac{\mu(N + A_d n \sigma_d) + C \tau_y (\phi) t \pi d \eta (1 - \phi)}{A_{pig}} \quad (3.25)$$

$$\Delta P_{pig} = \frac{17.4 \text{ kN}}{\frac{\pi 0.3^2}{4}}$$

$$\Delta P_{pig} = 2.5 \text{ bar}$$

This calculation assumes that the flowing oil works on the area equal to the pipe cross section. It does not include pressure loss due to a bypass system. By using equation 3.25 to calculate the pressure across the pig, the bypass flow rate can be found. Figure 12 shows how the bypass flow flushes away dislodged wax.

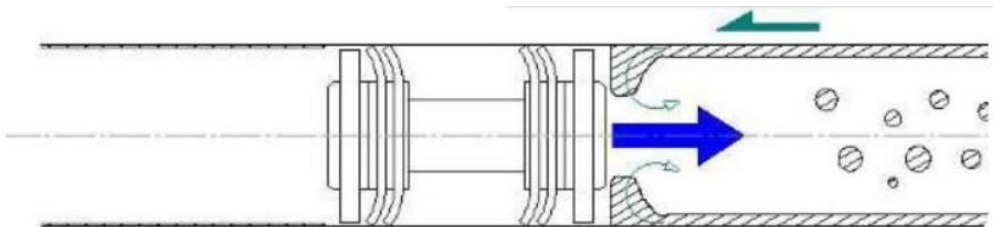


Figure 12: Wax removal with bypass pig (Skau, et al., 2013)

The coefficient of discharge C_d is a dimensionless number and is introduced for compensating for frictional losses, viscosity and turbulence effects. An often used value for the coefficient of discharge is 0.7. The bypass area varies from pig to pig, depending on the field of operation. In a paper by O'Donoghue (2004) it is used bypass ports that can vary the opening from 0.25 % by area and up to 2 % for his calculations (O'Donoghue, 2004). In a paper by Lee, et al, (2012) a bypass-area of 0 to 13 % has been used.

For a flowing fluid with density of 780 kg/m^3 and a differential pressure of 2.5 bar (calculated above) the bypass volume flow can be found. If the pipeline diameter is 0.3m and the bypass is set to 1 % the bypass area will be:

$$A_{bp} = \frac{\pi d^2}{4} \cdot \theta \quad (3.26)$$

$$A_{bp} = \frac{\pi \cdot 0,3^2}{4} 0.01 = 7.07 \cdot 10^{-4} \text{ m}^2$$

The bypass flow will then be:

$$q_{bp} = 0.7 \sqrt{\frac{2 \cdot 2.5 \cdot 10^5}{780}} \cdot 7.07 \cdot 10^{-4} = 0.013 \frac{\text{m}^3}{\text{s}}$$

O'Donoghue (2004) proposed a "Continuity Principle" to estimate the pig frequency of bypass size for a dewaxing pig. The principle states that the bypass flow rate should be greater than the rate of incoming wax, see equation 3.27. If this is being held, the wax accumulation will be prevented and wax gets flushed away (O'Donoghue, 2004). If the bypass rate is not adequate the wax may start to accumulate and form a plug. The volume flow of wax that needs to be flushed away can be estimated using Equation 3.28. Note that the wax removal efficiency for the pig affects the wax amount.

$$q_{bp} > q_{wax} \quad (3.27)$$

$$q_{wax} = u_{pig} A_{wax} \eta \quad (3.28)$$

The bypass system allows the operator to adjust the pig velocity. By changing the bypass area of the pig and let more flow through, the pig velocity decreases. From Southgate (2004) the equation for pig velocity is:

$$u_{pig} = \frac{u_{oil} A_{pipe} - C_d \sqrt{\frac{2\Delta P}{\rho}} A_{bp}}{A_{pipe}} \quad (3.29)$$

From the equation, pig velocity is dependent on the pressure differential across the pig. If the wax deposit layer increases in thickness, the removal forces will be higher. This gives a higher differential pressure needed and it results in a lower pig velocity.

To prevent a pig from stalling it is important to keep the pressure differential across the cleaning pig high. The flow rate is usually an operational constraint for the oil field. The differential pressure over the pig can be honed by decreasing the friction forces or altering the discharge coefficient of the bypass orifice (Southgate, 2004). If the flow rate is reduced for operational reasons it can lead to problems for a bypass pig. Reduced flow means that a larger fraction of the flow passes through the pig leading to less pressure build-up (O'Donoghue, 2002).

3.4 Pig effectiveness

The wax removal efficiency varies with the type of pig. Experiments done by Barros, et al, (2005) showed that the stiffer conical cup pigs and the hard disc pig had a wax removal efficiency of 100 %. All these pigs were assumed to apply to the load model 1, described in Chapter 4.2. In the same experiment, a disc pig with a more flexible disc was measured with an efficiency of 1 %. All the softer foam pigs did also have a rather poor efficiency. Also Wang, et al, (2005) reports different efficiency for the pig types. Although disc and cup pigs are made of the same material, the disc pig has a higher efficiency. On the other hand, the disc cup was observed to offer better durability and withstand higher loads. The foam pigs did have a poor efficiency in this test as well, but were less likely to get stuck in the pipeline. An interesting observation from the test is the effect of oil content in the mixture for the pig efficiency. For an oil content of 50 % in the deposit the wax removal efficiency was 100 % for a cup pig. When the oil content was reduced to 35 % the efficiency fell to 80.6 %. As the wax became harder, the removal efficiency was reduced (Wang, et al., 2005).

4 Pressure Drop Calculations

In a subsea pipeline transporting oil the inlet pressure will drop due to gravity, acceleration and friction. In this chapter the frictional pressure loss will be investigated for a pipeline suffering wax deposition. When the wax deposits on the pipe wall, the flow area for the oil decreases. This restricts the pipe flow and gives a pressure drop. The wall roughness does also change when wax deposits on the pipe wall. In this chapter pressure drop calculations will be presented.

4.1 Pressure Drop in Subsea Pipelines

The frictional pressure drop can be estimated using the Darcy-Weisbach equation (Equation 4.1). As seen from the equation, pressure drop is dependent on the friction factor. The Blasius friction factor correlation was used to calculate the pressure drop with wax deposition by Botne (2012). The Blasius formula does not account for the roughness value. To get realistic values, a friction factor formula that accounts for roughness is used in present calculations. In Haaland's equation, f is the friction factor, κ is the roughness in mm and n is a constant where n is 1 for fluids and 3 for gas. The pressure drop calculations in this thesis have been done analytical with Excel and properties from Table 9 is used.

$$\Delta P_f = \frac{f}{2} \frac{1}{d} \rho u^2 l \quad (4.1)$$

$$\frac{1}{\sqrt{f}} = -\frac{1.8}{n} \log \left[\left(\frac{6.9}{Re} \right)^n + \left(\frac{\kappa}{3.75d} \right)^{1.11n} \right] \quad (4.2)$$

From the master's thesis by Botne (2012) it can be seen that the pressure drop is inversely proportional to pipe diameter to the power of five. See equation 4.3. Because of this, it is expected that the pressure drop will have a large decrease due to the narrowing of the pipe.

$$\Delta P = \frac{f l}{2 d} \rho u^2 = \frac{f l}{2 d} \rho \left(\frac{4q}{\pi d^2} \right)^2 = \frac{8f l}{\pi^2 d^5} \rho q^2 \quad (4.3)$$

The flowing oil happens to be cooled down through the pipeline and as a result of this cooling process the properties of the oil changes. For the pipeline with properties used in present thesis the temperature goes from 45 C to around 7 C. The Reynolds number is dependent on both the viscosity and the density of the oil (Equation 2.8). This affects the pressure drop and has been taken into account for in the calculations. The oil density is also included in Equation 4.3 and should be looked at during pressure drop calculations. The viscosity and density change is found by using Hysys with the given oil composition, and is plotted against temperature in Figure 13 and Figure 14. An increase in viscosity leads to a lower Reynolds number and by this a higher friction factor. This should give a small increase in the pressure drop. The density of the composition increases as well. This gives a very small decrease in the friction factor. On the other side, the density is a factor in Equation 4.2, and this gives a much larger increase in pressure drop.

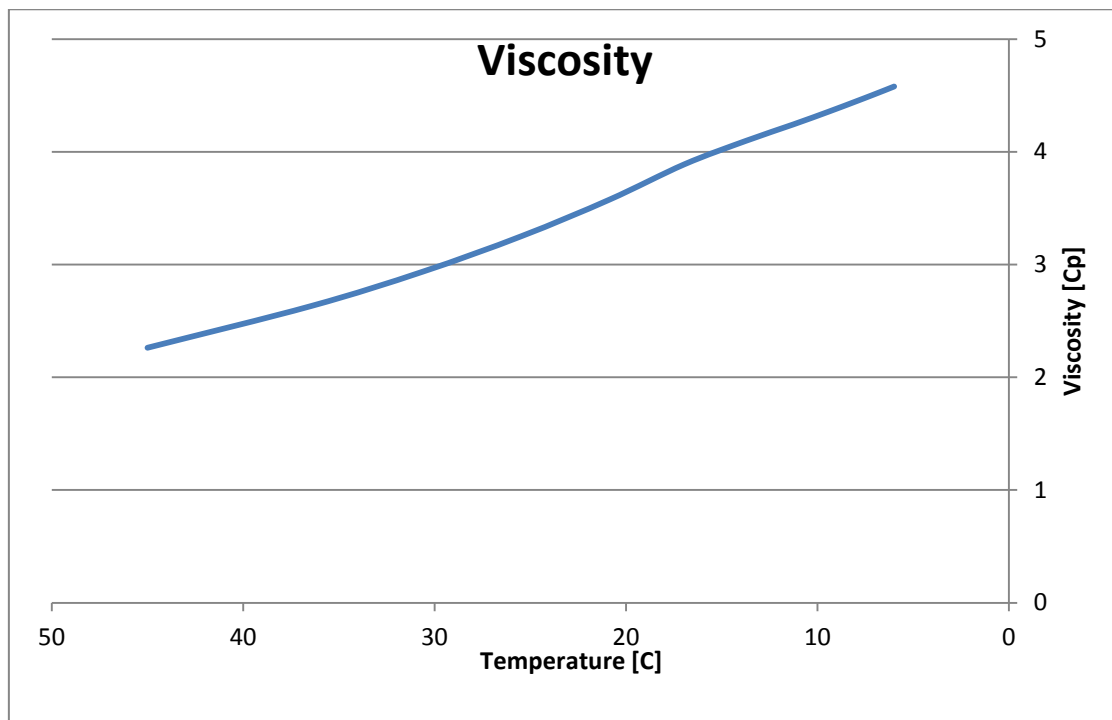


Figure 13: Viscosity vs. temperature for Norne oil composition

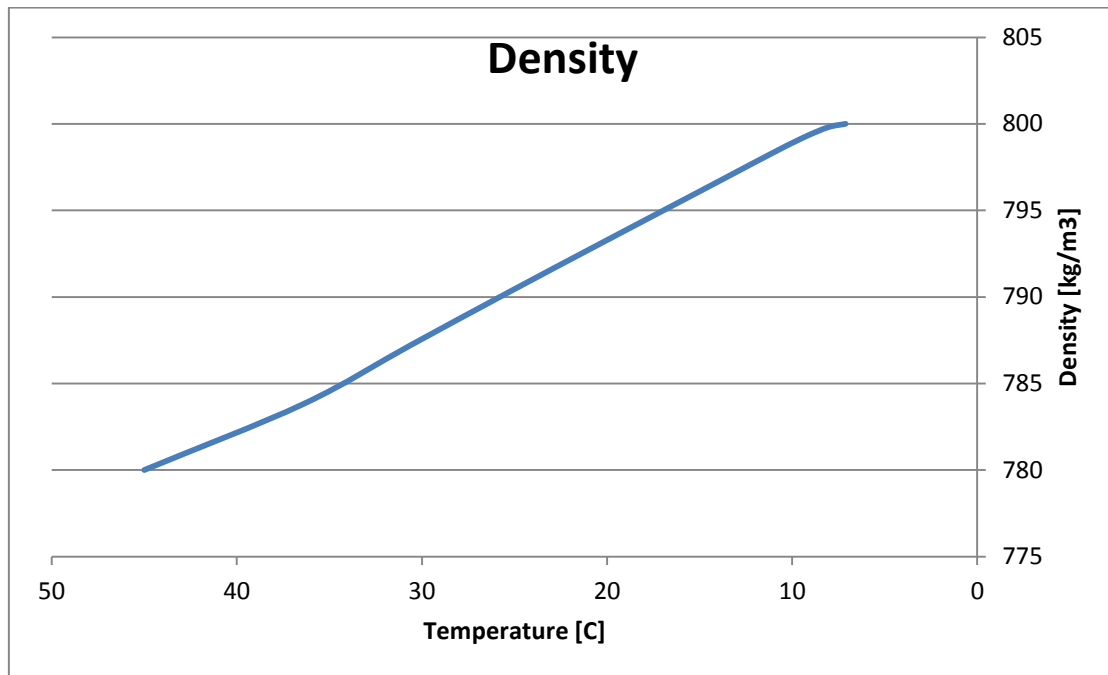


Figure 14: Oil density vs. temperature for Norne oil composition

4.2 Calculations with Focus on Wax Roughness

It is of interest to have a look at the pressure drop in a pipeline with and without wax deposition to see how the pressure drop changes. When wax deposits on the wall, the diameter will decrease. This affects the pressure drop for a pipeline. In addition the roughness of the pipe wall changes. In this chapter pressure drop calculations has been done to see the effect of roughness. By using the simulation software Hysys a wax deposition profile is found, and the values are used to calculate the pressure drop in excel. The deposition profile is shown in Figure 24.

The roughness value for wax deposit is of great importance when it comes to flow calculations in an oil pipeline. For pressure drop calculations the roughness must be known in order to achieve proper values. The Darcy-Weisbach equation is dependent on the friction factor. The roughness of bare steel varies in the literature, but from Gudmundsson (2009) an average absolute roughness value of 0.0351 mm is suggested. It is stated by Rønningsen (2012) that the local roughness of wax is equal to the local wax thickness, and with an upper limit of 7 mm. In the vast literature the roughness models for wax varies. It is proposed to use

a roughness of π -times the thickness of wax deposit layer for pressure drop calculations by Gudmundsson, see Appendix I.

To check how big the influence of the wax roughness has on the pressure drop, three calculation were done. The first one is done with the roughness held constant at the roughness value for mild steel ($35.1 \mu\text{m}$). The second calculation is done with a changing roughness that equals the thickness of the wax deposition. For the first part of the pipe, the roughness has the same value as for the bare steel. The wax deposition starts at 700 metres into the pipeline, and then the roughness value equals the wax deposition thickness. The third calculation is similar to the second one, but now the roughness value is set to the wax thickness multiplied with π . Properties of the fluid and the pipeline is presented in Table 9.

The results are plotted in Figure 15 and shows that the roughness has a significant effect on the pressure drop. For a roughness value of π -times the wax thickness, the shape of pressure drop curve gets very close to the shape of the wax profile. In comparison to the calculation with roughness in account, the decrease in pipe diameter does not affect the pressure drop as much as expected.

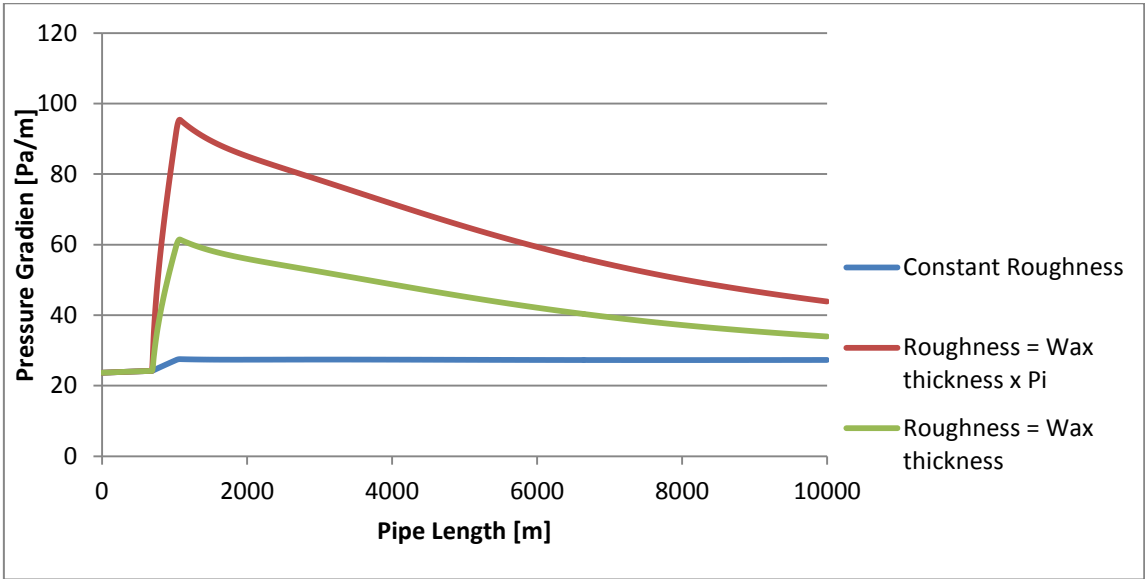


Figure 15: Pressure gradient for different values for roughness in a pipeline with wax deposition

The calculations show clearly that the major factor for the pressure drop gradient is the roughness. When the roughness value is held constant at the value for a steel pipe, the pressure gradient only has a minor increase when the wax build up begins. After the increase, the pressure gradient should be expected to follow the profile of the wax deposition. The gradient should therefore fall slowly as the wax thickness in the pipe decreases and the pipe

diameter increases towards the initial size. However, the pressure gradient seems to be constant through the rest of the pipeline. This can be explained by the viscosity and the density increase for the oil.

In the plot for the two calculations that accounts for the wax roughness, it can be seen that the pressure gradient drops after the maximum wax thickness. The reason for this is that the roughness decreases with the wax thickness. In addition the diameter plays a role for the curve. When the diameter increases again after the point of maximum wax thickness, the flow velocity decreases and so does the Reynolds number. However, also for the two last calculations the viscosity changes prevents an even steeper fall in pressure gradient.

The graph below in Figure 16 shows the calculated pressure drop for the pipeline. To check the numbers a simulation has been done in Hysys. The inputs used in the software simulations are taken from Table 9 and the oil composition is the same as in Chapter 2. The simulations are done with wax deposit and have the same wax profile as in Figure 24. The green plot in Figure 16 is the calculated pressure drop in Excel for the pipeline without wax deposition, meaning that the roughness is held constant at 35.1 μm and the pipe diameter at 0.3 m. The red line is the pressure drop from Hysys with wax deposition. The blue one is from Excel including wax deposition in the calculation. For the calculation with wax in the pipeline the pressure drops as expected where the wax thickness increases at 700 m into the pipeline.

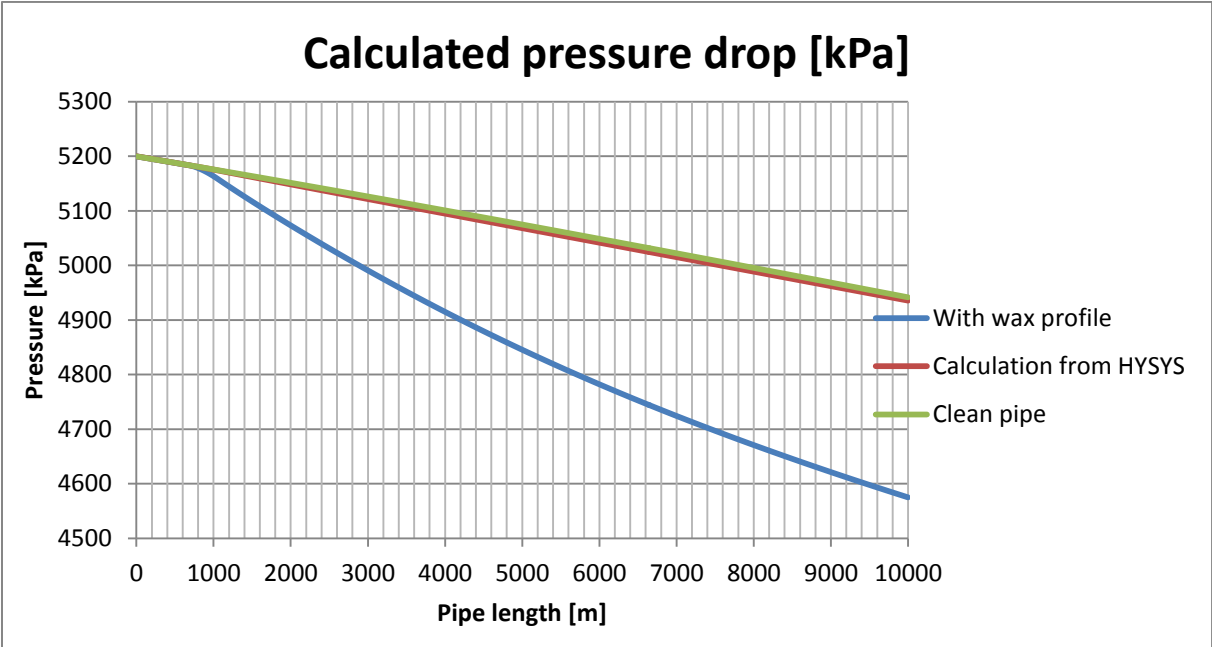


Figure 16: Calculated pressure drop for a clean pipe, with wax deposition and a Hysys simulation with wax

The interesting observation here is that the simulation from Hysys with wax deposition gives almost the same results as the calculations from Excel without wax deposition. A new simulation with Hysys has been done without wax deposition in the pipe, and the pressure drop estimation has shown to be the same.

The calculated pressure drop for a clean pipe is found to be 2.58bar, while Hysys is giving a value of 2.62 bar for the same pipeline with wax. This is an increase of 1.6 %. All three calculations follow the same gradient for the first 700 m, but then the curve for the calculation with wax profile falls. The total pressure drop for the wax profile case is 6.16 bar. This means that if the pipeline with wax deposit is pigged and all the wax is removed, the pressure drop is reduced by 3.58 bar. This number assumes that the pig has an efficiency of 100 % and the roughness returns to its initial state.

4.3 Calculations for Segmented Wax in Pipeline

The pressure drop in a pipeline differs if the wax deposit is non-evenly distributed.

Calculations using Excel has been done to check the pressure drop for a pipe with an evenly layer of wax deposit, and for two different cases with segmented wax layer as in the master's thesis by Botne (2012). The pressure calculations has been done with Equation 4.3, and the friction factor has been found using Equation 4.2. Table 9 shows the inputs for calculations.

For all calculations, the total amount of wax is held constant. By calculating the total volume of the wax profile in Figure 24 the amount is found to be 14.85 m³. This amount of wax is for the first calculation spread out as an evenly layer, giving a wax thickness of 1.57 mm. An evenly layer of wax deposit in the pipeline gives a pressure drop of 6.34 bar. For the parts of the pipeline without wax deposition, the roughness of bare carbon steel is used. For the parts with wax, the roughness is π -times the wax thickness. This can lead to very high roughness and friction factor numbers.

Assuming the same amount of wax distributed in 1/3 of the pipeline, the pressure drop is decreased to 5.48 bar. The wax starts at 700 m into the pipeline, but the total pressure drop is not affected by the location of the non-evenly distributed wax deposit (Botne, 2012). If the wax is deposit in 1/9 of the pipe, the pressure drop is 5.43 bar. To comparison, the pressure drop with the wax profile the pressure drop is 6.16 bar and is close to the results from the evenly distributed wax layer.

Results from this thesis shows that the largest pressure drop comes in a pipeline with an evenly distributed wax layer. If the amount of wax is distributed to 1/3 of the pipeline the pressure drop becomes smaller, while the smallest drop takes place in a pipe were the wax is distributed over 1/9 of the pipeline. See Table 1. These results differ from what was expected from Equation 4.2, when it comes to pressure drop due to diameter decrease. The results do also differ from the calculations done by Botne (2012). He has obtained results where wax distributed evenly gives lower pressure drop than wax segmented into a smaller part of the pipe. Results presented by Botne (2012) are shown in Figure 28.

Table 1: Results from pressure drop calculations

	Pressure drop [Bar]	Deviation [%]
Clean pipe	2.58	-
Pipe with wax profile	6.16	138
Pipe with evenly layer of wax	6.34	146
Pipe with a 1/3 distribution of wax	5.48	112
Pipe with a 1/9 distribution of wax	5.43	110

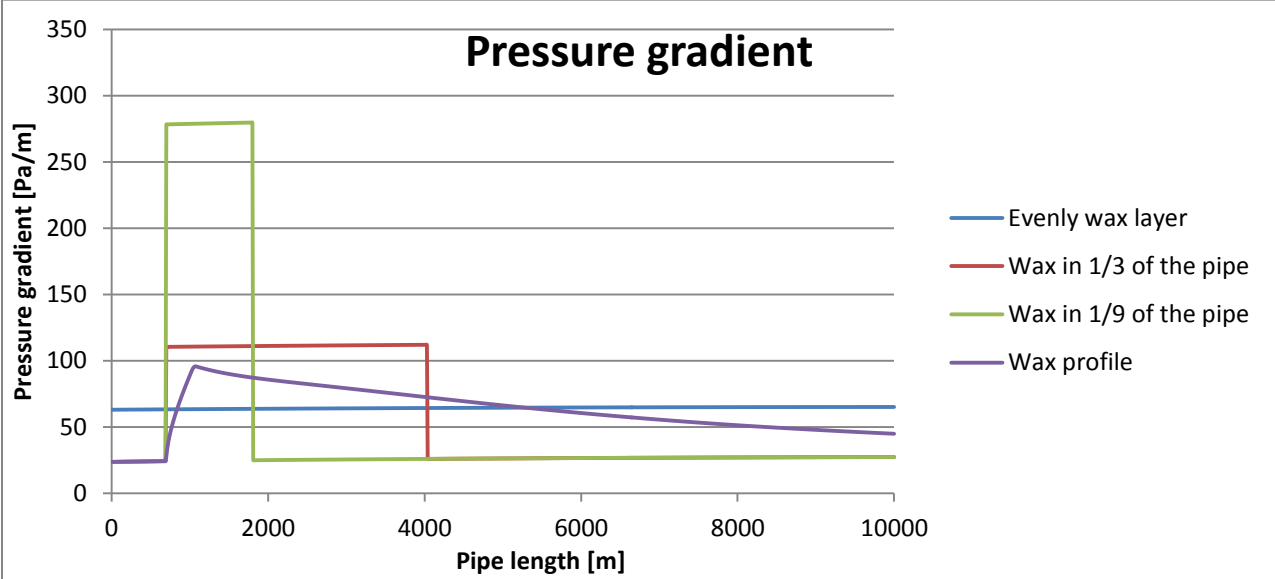


Figure 17: Pressure gradient for different wax distribution

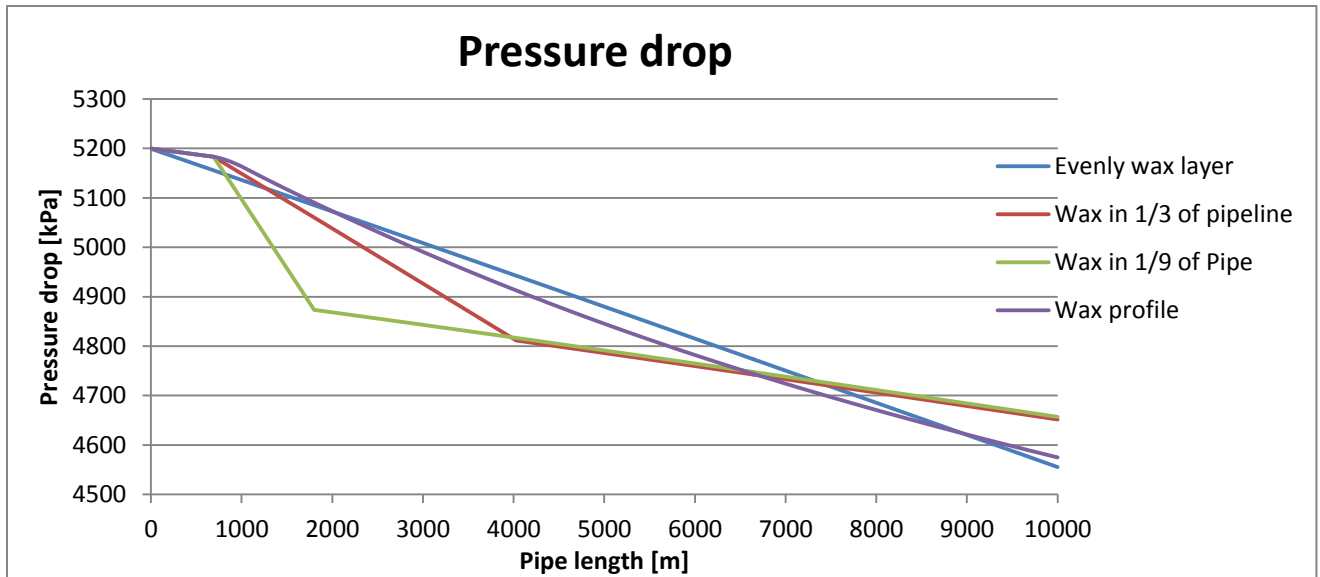


Figure 18: Pressure drop for different wax distributions

4.4 Calculations for Slurry Flow

The pressure drop in the pipeline downstream and upstream of the pig is different. Upstream the wall friction will be the steel roughness of the pipe, while downstream the wax layer gives higher roughness. In addition to the roughness, the viscosity changes as well. As a bypass pig moves through a pipeline the dislodged wax will be flushed in front of the pig. When particles are added to the bulk fluid the viscosity will change, as from Einstein's equation. From this equation the new mixture viscosity can be estimated if the wax particle fraction is known:

$$\mu = \mu_0(1 + 2.5\phi_{wax}) \quad (4.3)$$

As a calculation example, a maximum of 10 % dislodge wax can be handled in order to flush away the mixture. If a bare steel pipe is assumed the Darcy-Weisbach equation gives a pressure drop as showed in Table 1. The flow velocity is set to 1 m/s. The viscosity is changing with the amount of wax in the solution and Einstein's equation is used. Haaland's friction formula is dependent on Reynolds number and gives higher values for the friction factor for more viscous fluids. The first calculation is done with a pipeline without wax deposition, while the second one is done the wax profile shown in Figure 24. The results for the calculations can be seen in Table 2 and Table 3.

Table 2: Pressure drop for slurry flow and clean pipe

	Pressure drop [bar]	Deviation [%]
Pure oil	2.58	-
Oil with 10% wax	2.69	4.3
Oil with 50% wax	3.03	17.4

Table 3: Pressure drop for slurry flow and wax deposition

	Pressure drop [bar]	Deviation [%]
Pure oil	6.16	-
Oil with 10% wax	6.17	0.2
Oil with 50% wax	6.21	0.8

For the second calculation the deviation is way smaller and is not a major factor for the total pressure drop in the pipe. This calculation is done for the entire pipeline, while under a pigging operation the length of the pipe that is affected by the slurry flow decreases with time.

4.5 Calculations of Pressure Drop under Pigging Operation

There is a large difference for the pressure drop with and without wax deposition. From Chapter 4.2 the pressure drop with the simulated wax profile is 140 % higher than for a clean pipe. When a pig is moving through the pipe, wax is removed from the wall and the pressure gradient changes. This subchapter presents pressure drop calculations for a pipeline when a bypass cleaning pig is in operation.

The oil flow rate in the pipeline is assumed to be constant, and the pig velocity varies with the differential pressure across the pig. The resistance the pig meets through the pipeline varies with the wax thickness. This changes the differential pressure and the pig velocity. The pig velocity is calculated with Equation 3.28 and is plotted against the pipe length in Figure 27. As can be seen, the pig velocity change is very small. Table 10 gives more properties needed to do the calculations in this chapter.

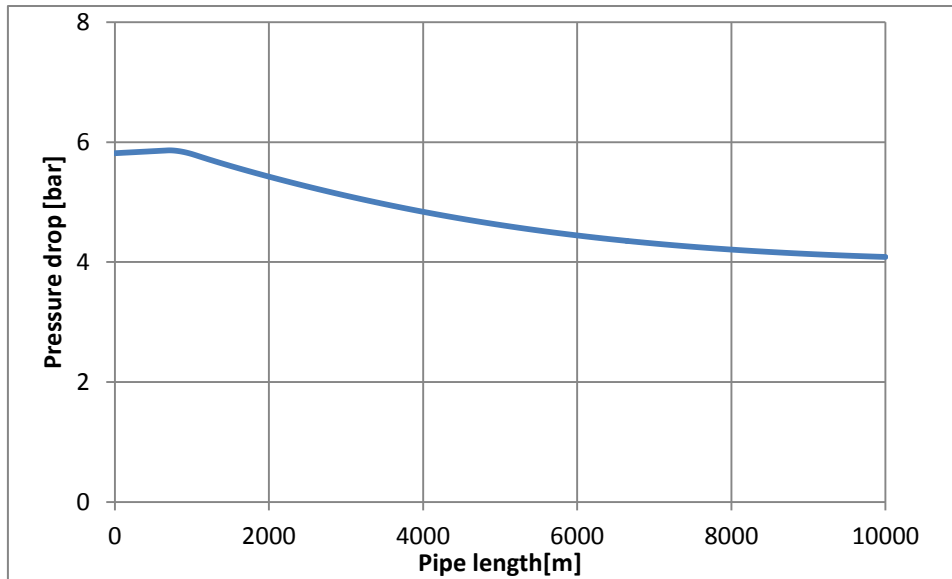


Figure 19: Pressure drop in the pipeline including pressure drop across pig

The figure above shows the total pressure drop over a pipeline while the pig is in operation. The graph is plotted for the position for the pig along the x-axis. At start, the pressure drop is just below 6 bar, including 2.5 bar drop over the pig. As the pig moves through the pipeline removing wax from the wall, the pressure drop sinks. When the pig is at 4000 metres into the pipeline, the total pressure drop for the pipeline is approximately 5 bar.

The graph below in Figure 20 shows the pressure curve for a pipeline when a pig is halfway through the line. Upstream of the pig the pressure falls almost linearly down. The oil flow rate is $0.071 \text{ m}^3/\text{s}$ and the pig velocity is changing with the differential pressure. Equation 3.23 is used to calculate the bypass flow as the pig moves through the pipe. Because of the bypass, the fluid has a slightly higher velocity than the pig. Downstream of the pig the pipeline contains wax and therefore the diameter is decrease. In addition a small amount of wax is added to the flow. The amount of wax added to the flow is estimated from Equation 3.28. The flow rate in front of the pig is assumed to be the sum of the flow rate needed to keep the pig velocity in addition to the bypass rate. Equation 4.4 describes the flow rate downstream of the pig. The viscosity does also change with the amount of wax removed from the pipe wall, as calculated in Chapter 4.4. This, in addition to the higher roughness value for wax gives a steeper pressure drop downstream of the pig as seen below in Figure 20.

$$q_{down} = u_{pig}A_{pw} + q_{wax} \quad (4.4)$$

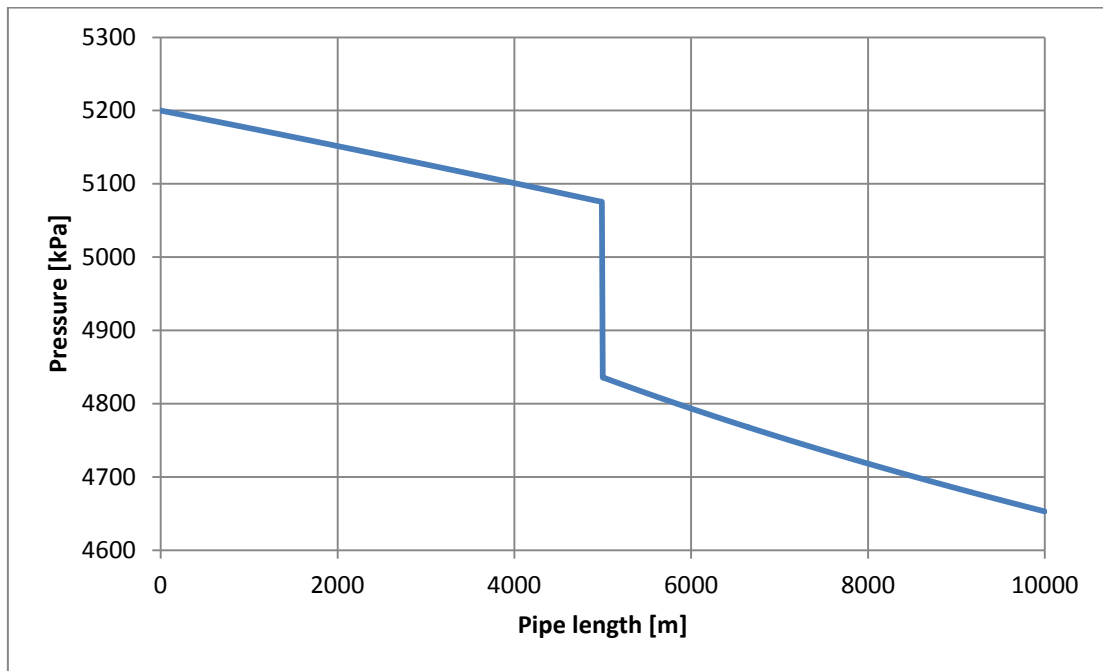


Figure 20: Pressure profile with pig half way in pipeline

5 Discussion

The knowledge about the overall heat transfer coefficient is important for prediction the wax deposition of a pipeline and finding the pigging frequency. The increase in U-value for the pipeline gives a decreased growth for the wax deposition. This means that the area of wax in the pipeline gets smaller. For pigging frequency, this should mean that pigging operations should happen less often. However, the forces of newly deposited wax are small compared to old hardened wax. For the pigging frequency, it is important to pig often to prevent ageing of the wax in the pipeline.

5.1 U-value Calculations

The calculations done for the overall heat transfer coefficient are based on properties for a typical subsea pipeline. The estimations will not be as accurate as for a real pipeline, but the numbers achieved gives a clear indication. The calculations are done with one set of properties, and the results may not be transferred to other pipelines with different properties.

The results from this thesis show that the wax thickness has an insulating effect. The overall heat transfer coefficient has a large decrease because of the added wax layer. The result does also show that when other factors have a large impact on the U-value, the effect of the wax layer is not as extensive. In these calculations, a partly or fully buried pipeline is not considered. It is conceivable for this results that the insulating effect of wax deposition is even smaller for a buried pipeline. This corresponds well with the conclusion by Christiansen, 2011.

Results from the analytical calculations give similar results as by Christiansen (2011). His results for calculations of the U-value for increasing wax thickness are shown in Figure 26. The small variations in results are assumed to be because of different oil composition. Also the seawater properties have been changed slightly. For a clean pipe without wax deposition the results correspond well between Hysys and the analytical calculations. The overall heat transfer coefficient estimated by Hysys is 5 % higher than for the analytical calculation.

A test has been done to see if the simulation software Hysys do account for wax deposition when estimating the U-value. The results in Hysys for U-value estimation are the same with

and without wax deposition in the pipeline for simulations done in this thesis. This means that Hysys do not account for the insulating effect when the U-value is estimated. The results in this thesis are based on only a few simulations, and with only one set of parameters. The simulations are also only based on one version of the software, V.8.3. If this results shows to be the case for other users of the software, it is a big weakness that should be investigated further. When the overall heat transfer coefficient is estimated higher than in reality, the wax deposition will be over predicted.

In addition to the wax insulation test, Hysys has been tested for the flow velocity as well. Results show that Hysys do account for the flow velocity when estimating the overall heat transfer coefficient. As presented in chapter 2.1 a higher flow velocity means a higher value for the overall heat transfer coefficient. This makes the U-value estimation in Hysys a bit more accurate.

5.2 Pigging Principles

In this thesis forces for friction and wax removal is presented. The information can be used as a basic model for illustrating the acting resistive forces for a pig in operation. None of the force values estimated in this thesis can be directly transferred to another pipe system. The properties for the oil/condensate flow must be known, in addition to the pipe and environmental properties, to be able to give reasonable values.

Equation 3.7 is developed by the author and is based on theoretical assumptions for how the physics must work for a pig in a pipeline. It is not been tested in real life, and has not been used in a simulation software. The equation does however give results that are in the same order of magnitude as the contact forces mentioned by Nieckele, et al, (2001). This does not mean that the equation is correct, but it may have a potential for describing the forces that acts on a pig in operation. It should also be mentioned that the numbers given by Nieckele, et al, (2001) is based on only one type of high friction bi-directional pig. In order to validate the credibility of Equation 3.7, real experiments should be done.

A frictional force of 16.5 kN is calculated and presented in the thesis for the given pipe diameter. This can give an indication for how large the forces are for friction between the pig and the pipe wall. This friction force is based on many factors that can vary. The coefficient of friction is one of them. In present calculations a value of 0.4 is used, but it is difficult to

obtain realistic numbers without real test data. As mentioned in chapter 3.1, the oversize value of the cleaning disc seems to be the most important factor for the second term of Equation 3.7. In addition, the width and the number of discs on the pig give different values.

Equation 3.7 does not account for pig velocity and how the discs act when the pig moves. When in motion the discs may buckle and give less resistive force due to oversize. A much lower value for the friction is presented by Botros & Golshan, 2010. They state that the frictional force is dependent on pig velocity, as in Equation 3.11. This is for an inspection pig tool. These types of pigs have a different structure and may have way lower frictional forces than dewaxing cleaning discs.

It was claimed by Barros, et al, (2005) that wax deposition can be the most important factor when it comes to pig stalling. Results from the paper say that the resistive forces by the wax can be three times as large due to wax accumulation in front of the pig. When bypass introduced, the problem may be reduced. In earlier literature, the focus has often been on only the thickness of wax. An investigation is done for the forces for wax removal in present thesis. By having a larger focus on the wax properties, more accurate removal forces can be achieved. It is shown that a higher wax content of the deposit leads to higher removal forces. Ageing of the wax leads to a lower oil/condensate content of the wax, and the deposit hardens over time. In addition, the adhesion force plays an important role. These properties should be further investigated. It would be of great interest to find a method of predicting the adhesion and ageing properties.

Numbers given in this thesis says that frictional forces are much higher than the wax removal forces. It should still be a large focus on the wax forces. As mentioned above, the ageing of wax leads to hardening of the deposit. This increases the wax removal forces, but it may also have an impact on the pig efficiency. If the material of the pig discs is too soft, and the wax is too hard, the pig will start to ride over the deposit. This applies to load model 2 as is explained in Chapter 3.2, where the pig efficiency is drastically reduced.

For the pigging frequency, it does not seem like the thickness of wax is very important, if not the effect of ageing and adhesion is considered. The growth of wax will continue for each day without pigging, until it stagnates because of the deposition driving force. If the rate of ageing is known, this should be considered when choosing the pigging frequency. The wax will harden with time, and pigging should happen often to prevent that. If the removal efficiency of the pig decreases, it means that pigging must happen even more frequent to remove all the deposit.

5.3 Pressure Drop Calculations

In Chapter 4.2 pressure drop calculations has been done to see the effect of roughness for wax deposition. It is expected from Equation 4.3 that the decrease in pipe diameter due to wax deposition will have a large influence on the pressure drop. However, it seems like the roughness of the deposits is the dominating part. A roughness value of π -times the wax thickness is used. This will give very high values for the roughness when the deposit thickness is at its peak.

The density of oil composition increases from 780 to 800 kg/m³ through the pipe in present thesis. For the result for constant roughness in Figure 15, the gradient where expected to fall because of the diameter in Equation 4.3. The density increase prevents this and keeps the curve in a straight line. The viscosity and density change affects the Reynolds number and gives a higher friction factor. This increase keeps the pressure gradient from falling.

The numbers calculated with Excel was supposed to be compared to the simulated pressure drop with Hysys. The results in this thesis show that Hysys estimated the pressure drop with and without wax deposit to be the same. The same limitations as described in Chapter 5.1 are applicable. Hopefully this it is just an error concerning my version of the software. Otherwise it will be yet another weakness for Hysys.

Figure 16 shows the total pressure drop for the analytical calculations with and without wax deposition. It shows that when the wax layer starts at 700 metres into the pipe, the pressure falls. The pressure drop for a pipeline after pigging will be reduced by 3.58 bar if the pigging efficiency is 100 %. If the pig does not have a 100 % wax removal efficiency, the roughness in the pipe can vary if wax is still present in the pipe wall. This can lead to a higher pressure drop for the pipeline than expected after pigging.

How segmenting of the way deposit in a pipeline will affect the pressure drop is shown in Figure 17 and Figure 18. The results for segmented wax deposition by Botne (2012) differ from the results in present thesis. One reason can be that a much higher value for the roughness is used in present thesis. In addition, present thesis uses a lower volume of wax. This gives less decrease in diameter for the pipeline. This can mean that the friction factor have a bigger influence on the pressure drop than the diameter decrease for high roughness values.

For slurry flow calculations the wax particles in oil does not affect the pressure drop much for a pipe with wax deposition. In addition, the slurry flow situation will only affect the pressure drop for a small part of the pipeline in the end of a pigging operation. It is more important to look at the difference for the pressure gradient upstream and downstream of a pig. The pressure drop in the pipeline is at its maximum when the pig is around 700 m. This is when the pig approaches the peak of the wax deposits. The flow rate used in the calculations is fairly low. The pig velocity is usually higher than 0.8 m/s, as found in the calculations. A higher pressure drop would be achieved if the pig flow velocity was higher.

6 Conclusion

- In this master's thesis it has been shown that wax deposit has an insulating effect in a subsea pipeline. Estimation of the overall heat transfer coefficient has been done with Hysys. Results show that Hysys do not account for the simulated wax deposit when estimating the U-value for a subsea pipeline. On the other hand, Hysys do account for changing flow velocity in the pipeline when estimating the U-value.
- The strength of wax is dependent on the oil/condensate content and how the wax adheres to the wall. Ageing of wax leads to higher wax removal forces, and the removal efficiency of the pig may decrease. Pigging of the pipeline must happen at a given frequency to prevent the wax from hardening.
- It has been presented a model for a bypass cleaning pig in operation in this thesis. Assumptions have been done to calculate the frictional forces and the wax removal forces. Results in this thesis shows that the frictional forces due to contact between cleaning discs and the pipe wall are higher than the forces for wax removal. There are many factors that affect the contact forces for a pig, and it is difficult to find realistic number without experimental data for the real pipeline system.
- Pressure drop calculations for a pipeline with wax deposition have been done. Results show that the roughness value for the wax layer has a large influence on the pressure drop. A pigging operation reduces the pressure drop in the pipeline if the pig efficiency is high.

7 Further Work

It should be done investigations of the effect ageing has on the strength of the wax deposit. In order to give accurate predictions for the wax removal forces at a given pigging frequency, the strength of the wax need to be known. More knowledge about how the wax adheres to the pipe wall is of interest when finding the wax removal forces.

An expression for the frictional force between the pig and the pipe wall has been given in this thesis. The equation should be tested against real experiments to check the credibility of the expression.

The wax scraping tool on the pig can be enhanced. A claim stated by Southgate (2004) says there is a potential in using more efficient tool geometry for scraping the wax. The pig form factor ϕ can be lowered to reduce the wax removal forces for a dewaxing pig.

8 References

Azevedo, L. F. A., Braga, A. M. B., Nieckele, A. O. & Naccache, M. F., 1996: Simple Hydrodynamic Models for the Prediction of Pig Motions in Pipelines. Offshore Technology Conference, May, Houston, 11 pp.

Bai, Y. & Bai, Q., 2005. Subsea Pipelines and Risers, Oxford, Elsevier, 919 pp.

Bai, Y. & Bai, Q., 2010. Subsea Engineering Handbook. Houston, Elsevier, 812 pp.

Barros, J. M., Alves, D.P.P., Barroso, A.L., Souza, R.O. & Azevedo, L.F.A., 2005. Experimental Validation of Models for Prediction Wax removal Forces in Pigging Operations. Rio de Janeiro, 18th International Congress of Mechanical Engineering, November 6-11, 8 pp.

Botne, K. K., 2012. Modeling wax thickness in single-phase turbulent flow. Master`s thesis, Department of Petroleum Engineering and Applied Geophysics, NTNU, June, Trondheim, 70 pp.

Botros, K. K. & Golshan, H., 2010. Field Validation of a Dynamic Model for an MFL ILI Tool in Gas Pipelines. ASME, Proceedings of the 8th International Pipeline Conference, Calgary, Alberta, September 27 – October 1, 12 pp.

Christiansen, H. E., 2011. Temperature profile in subsea pipelines. Specialization Project, Department of Petroleum Engineering and applied Geophysics, NTNU, December, Trondheim, 41 pp.

Davidson, R., 2002. An Introduction to Pipeline Pigging. Pigging Products and Services Association, PPSA Aberdeen Seminar, Aberdeen, 10 pp.

Fahre-Skau, A., O'Donoghue, A., Rønningsen, H. P., Rongved, K., 2013. Heimdal Brae De-Waxing Operation, PPSA Seminar 20th November, URL: <http://ppsa-online.com/papers/13-Aberdeen/2013-05-Statoil-slides.pdf>. Date accessed: 28.05.2014.

Galta, T., 2013. Pigging Operations in Subsea Pipelines Suffering Wax Deposition. Specialization project, Department of Petroleum Engineering and Applied Geophysics, NTNU, Trondheim, 37 pp.

Gudmundsson, J. S., 2009. Prosessering av Petroleum, Kompendium TPG4135. Department of Petroleum Engineering and Applied Geophysics, NTNU, April, Trondheim, 181 pp.

Hossain, E. M., Chafi, K. & Islam, R. M., 2009. Experimental Study of Physical and Mechanical Properties of Natural and Synthetic Waxes Using Uniaxial Compressive Strength Test. Proceedings of the Third International Conference in Modeling, Simulation and Applied Optimization, January 20-22, Sharjah, 5 pp.

Hovden, L., Xu, Z.G., Ronningsen, H. P., Labes- Carrier, C. and Rydahl, A., 2004. Pipeline Wax Deposition Models and Model for Removal of Wax by Pigging: Comparison between Model Predictions and Operational Experience. 4th North American Conference on Multiphase Technology, 3-4 June, Banff, Canada 20 pp.

Lee, H. S., Agustiawan, D., Jati, K. & Aulia, H. M., 2012. By-pass Pigging Operation Experience and Flow Assurance Study. Offshore Technology Conference, 30 April – 3 May, Texas, 10 pp.

Mendes, S. R. P., Braga, A. M. B., Azevedo, L. F. A. & Correa, K. S., 1999. Resistive Force of Wax Deposits During Pigging Operations. ASME, Journal of Energy Resources Technology, September, Vol. 121, pp 167-171.

Nieckele, A. O., Braga, A. M. B. & Azevedo, L. F., 2001. Transient Pig Motion Through Gas and Liquid Pipelines. ASME, Journal of Energy Resources Technology, December, Vol. 123, pp 260-269.

Norsk Standard, 2006. Norsok Standard P-001, Process design. Edition 5, September, Lysaker, 22 pp.

O'Donoghue, A., 2002. Why pigs get stuck and how to avoid it. Pipeline Pigging Conference, Amsterdam, October, 16 pp.

O'Donoghue, A., 2004. Pigging as a Flow Assurance Solution Estimating Pigging Frequency for Dewaxing. Pipeline Pigging Conference, Amsterdam, May, 10 pp.

Pipeline Research, 2002. URL: <http://www.pipeline-research.com/HighFrict.html>, Date accessed: 24.05.2014.

Rønningsen, H. P., 2012. Production of Waxy Oil on the Norwegian Continental Shelf: Experiences, Challenges, and Practices. ACS Publications, Energy and Fuels, May 18, pp 4124-4136.

Seyfaee, A., Lashkarbolooki, M., Esmailzadeh, F. & Mowla, D., 2012. Investigation of the Effect of Insulation on Wax deposition in an Iranian Crude Oil Pipeline with Olga Simulator. Journal of Dispersion Science and Technology, 33:8, pp 1218 – 1224.

Siljubergh, M. K., 2012. Modelling of Paraffin Wax in Oil Pipelines. Master's thesis, Department of Petroleum Engineering and Applied Geophysics, NTNU, July, Trondheim, 68 pp.

Southgate, J., 2004. Wax Removal using pipeline pigs. PhD's thesis, Durham University, Durham E-Theses Online: <http://etheses.dur.ac.uk/2995/>, June, 269 pp.

SPT-Group. Olga User Manual, version 7.0, 2011. 513 pp.

Wang, Q., Sarica, C. & Chen, T. X., 2005. An Experimental Study on Mechanics of Wax Removal in Pipeline. ASME, Journal of Energy Resources Technology, December, Vol. 127, pp 302-309.

Wu, H. L. & Spronsen, G. v., 2005. Slug reduction with high by-pass pigs - a mature technology. 12th International Conference on Multiphase Production Technology, May 25-27, Barcelona, Spain, pp 313-325.

Zhang, X., Queimada, A., Szczepanski, R. & Moorwood, T., 2014. Modeling the Shearing Effect of Flowing Fluid and Wax Ageing on Wax Deposition in Pipelines. Offshore Technology Conference Asia, 25-28 March, Kuala Lumpur, Malaysia, 22 pp.

Tables

Table 4: Properties for U-value calculations

Pipe length	12000	m
Inner pipe diameter	0.305	m
Outer diameter, steel	0.329	m
Outer diameter, concrete	0.380	m
Steel thickness	0.012	m
Concrete thickness	0.025	m
Mud thickness	0.015	m
Inlet temperature	45	C
Inlet pressure	52	Bar
Ambient seawater temperature	5	C
Volume rate	255	m ³ /s

Table 5: Thermal conductivity

Wax	0.25	W/m·K
Oil	0.2596	W/m·K
Steel	20	W/m·K
Concrete	1.5	W/m·K
Sea water	0.65	W/m·K
Mud	0.6	W/m·K

Table 6: Fluid properties

Density, oil	764.6	kg/m ³
Density, sea water	975.6	kg/m ³
Flow velocity, oil	1.0	m/s
Flow velocity sea current	0.1	m/s
Heat capacity, oil	2416	J/kg·K
Heat capacity, sea water	4200	J/kg·K
Viscosity, oil	1.42	mPa·s
Viscosity, sea water	1.88	mPa·s

Table 7: Assumed oil composition for the Norne field

Component	Mass fraction [%]	Component	Mass fraction [%]
C1	0.14	C27	3.13
C2	0.16	C28	2.14
C3	0.3	C29	2.10
C4	0.60	C30	1.48
C5	0.65	C31	1.66
C6	0.90	C32	1.73
C7	2.51	C33	1.53
C8	4.47	C34	1.28
C9	3.41	C35	1.28
C10	2.87	C36	1.03
C11	2.78	C37	0.88
C12	3.07	C38	0.84
C13	3.82	C39	0.80
C14	4.26	C40	0.64
C15	4.52	C41-45	2.81
C16	3.75	C46-50	1.90
C17	4.63	C51-55	1.37
C18	3.83	C56-60	1.03
C19	3.75	C61-65	0.76
C20	3.29	C66-70	0.57
C21	3.26	C71-75	0.47
C22	2.75	C76-80	0.31
C23	2.97	C81-85	0.29
C24	2.35	C86-90	0.23
C25	2.21	C91-95	0.23
C26	2.14	C96-100	0.14

Table 8: U-value results from simulations with Hysys

	Overall HTC (OD)	Overall HTC (ID)	U-Value	Inlet temp
Pipe segment	$\text{kJ/h}\cdot\text{m}^2\cdot\text{K}$	$\text{kJ/h}\cdot\text{m}^2\cdot\text{K}$	$\text{W/m}^2\cdot\text{K}$	C
1	164.66	208.35	57.9	45.0
2	162.65	205.80	57.2	38.7
3	161.07	203.81	56.6	33.4
4	160.00	202.45	56.2	28.9
5	159.47	201.79	56.1	25.1
6	159.12	201.34	55.9	21.9
7	158.87	201.03	55.8	19.2
8	158.70	200.81	55.8	16.9
9	158.59	200.67	55.7	15.0
10	158.51	200.57	55.7	13.4
11	158.46	200.51	55.7	12.0
12	158.43	200.46	55.7	10.9

Table 9: Properties for pressure drop calculations

Inlet temperature, T	45 C
Inlet pressure, P	52 Bar
Inner diameter, d	0.3 m
Pipe length, L	10000 m
Inlet flow velocity, u	1 m/s
Flow rate, q	0.071 m ³ /s
Roughness clean pipe, κ	35.1 μm
Overall heat transfer coefficient, U	20 $\text{W/m}^2\cdot\text{K}$
Fluid density, ρ	780 kg/m^3
Fluid viscosity inlet, μ	2.14 Cp
Reynolds number inlet	109805

Table 10: Properties for pressure drop calculations with pig

Bypass area fraction	1	%
Bypass area	0.00071	m ²
Discharge coefficient, Cd	0.7	
Differential pressure, ΔP	2.6	Bar
Oil flow rate, q_{oil}	0.071	m ³ /s
Oil velocity, u_{oil}	1	m/s
Bypass rate, q_{bp}	0.013	m ³ /s
Pig velocity, u_{pig}	0.83	m/s
Wax removal efficiency for pig, η	100	%
Oil content in wax, ϕ	30	%

Table 11: Properties for wax removal forces

Pipe diameter, d	0.3	m
Yield stress, τ_y	0.28	MPa
Wax breaking force coefficient, ϕ	$\sqrt{2}$	
Wax removal efficiency for pig, η	0.95	
Pig form factor, φ	0	

Figures

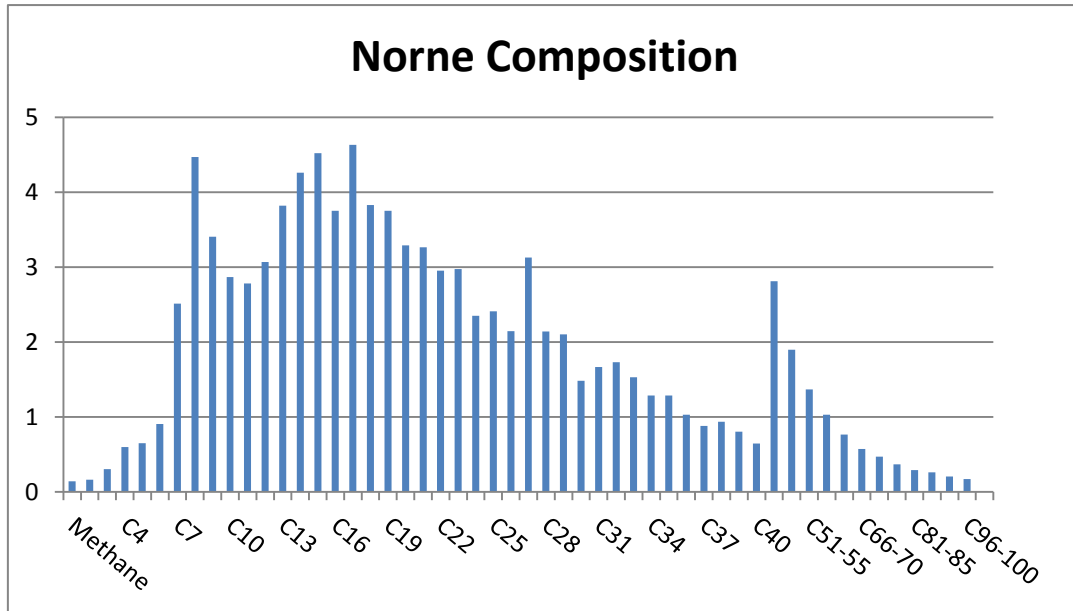


Figure 21: Norne composition (Galta, 2013).

Heat Transfer Coefficient Estimation

Ambient Temperature:

Include Pipe Wall: Global By Segment

Include Inner HTC: Correlation

Include Insulation: Insulation Type
 Thermal Conductivity
 Thickness

Include Outer HTC: Ambient Medium
 Velocity

Figure 22: Inputs in Hysys for heat transfer coefficient estimation

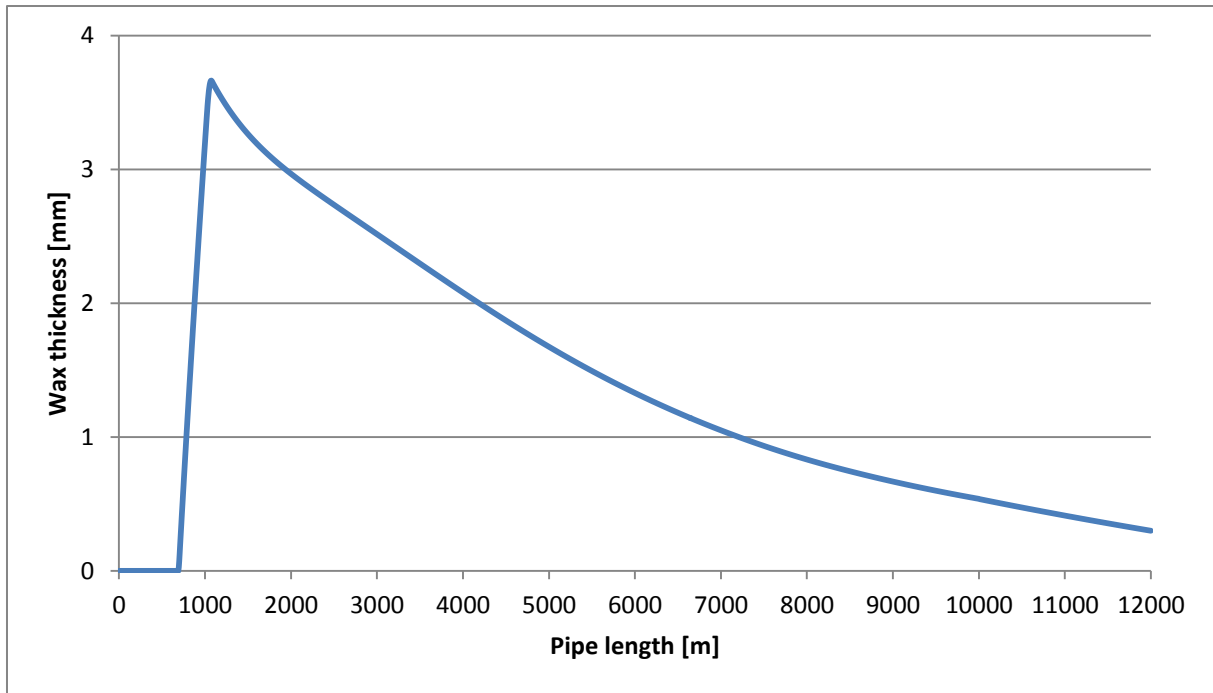


Figure 23: Wax deposition profile for Hysys U-value estimation

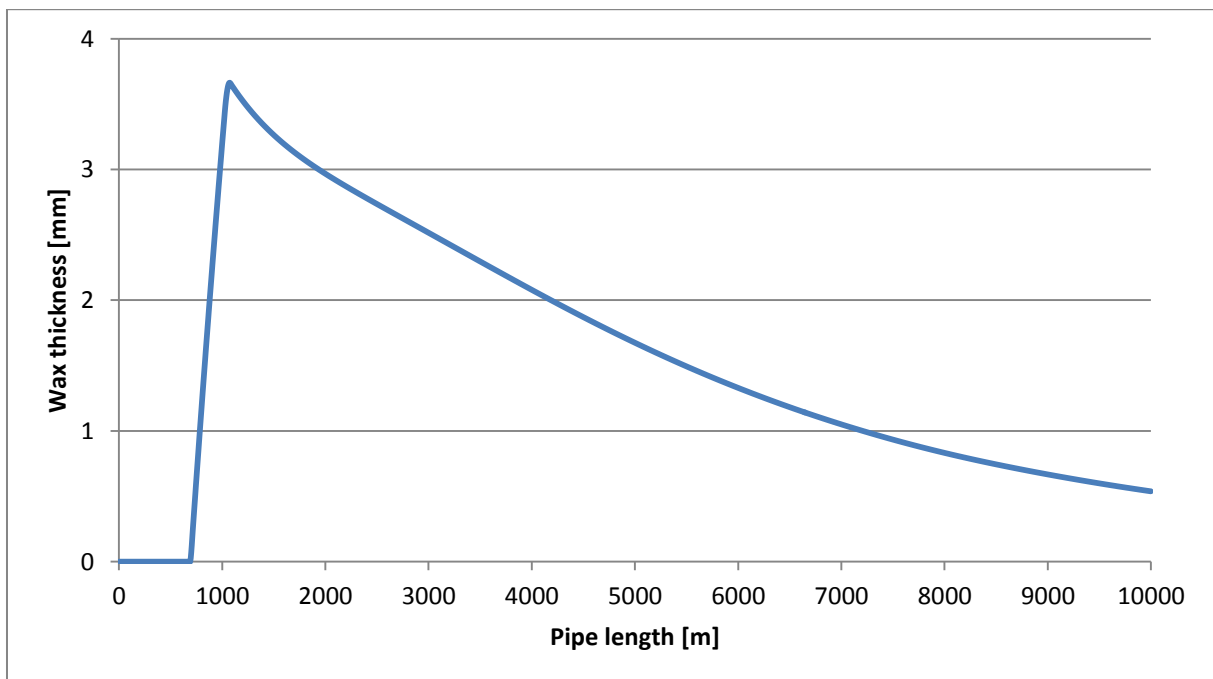


Figure 24: Wax deposition profile for pressure drop calculations

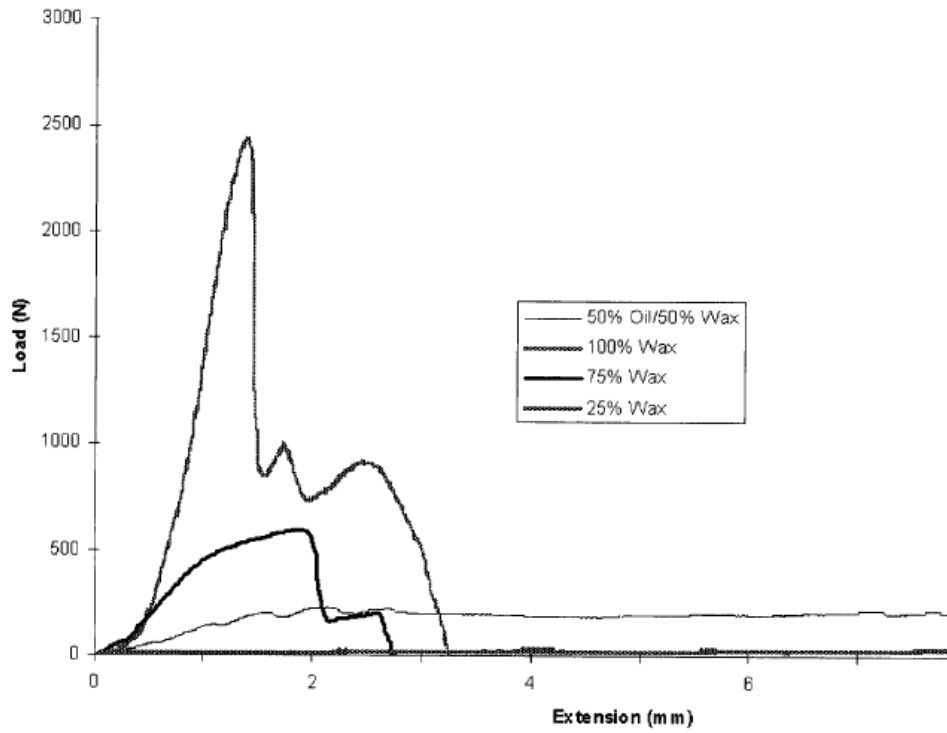


Figure 25: Load vs. extension graph for various oil content wax samples. (Southgate, 2004).

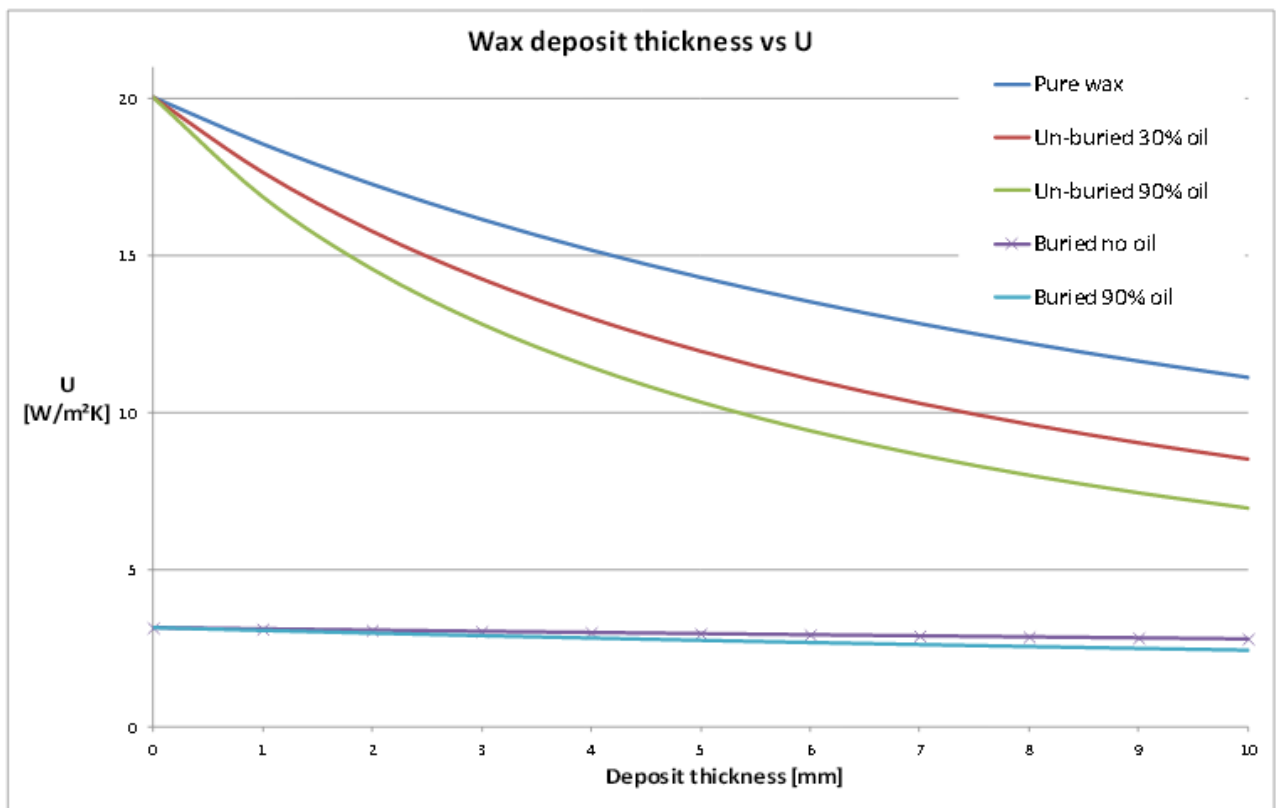


Figure 26: Wax deposit thickness vs. U. (Christiansen, 2011)

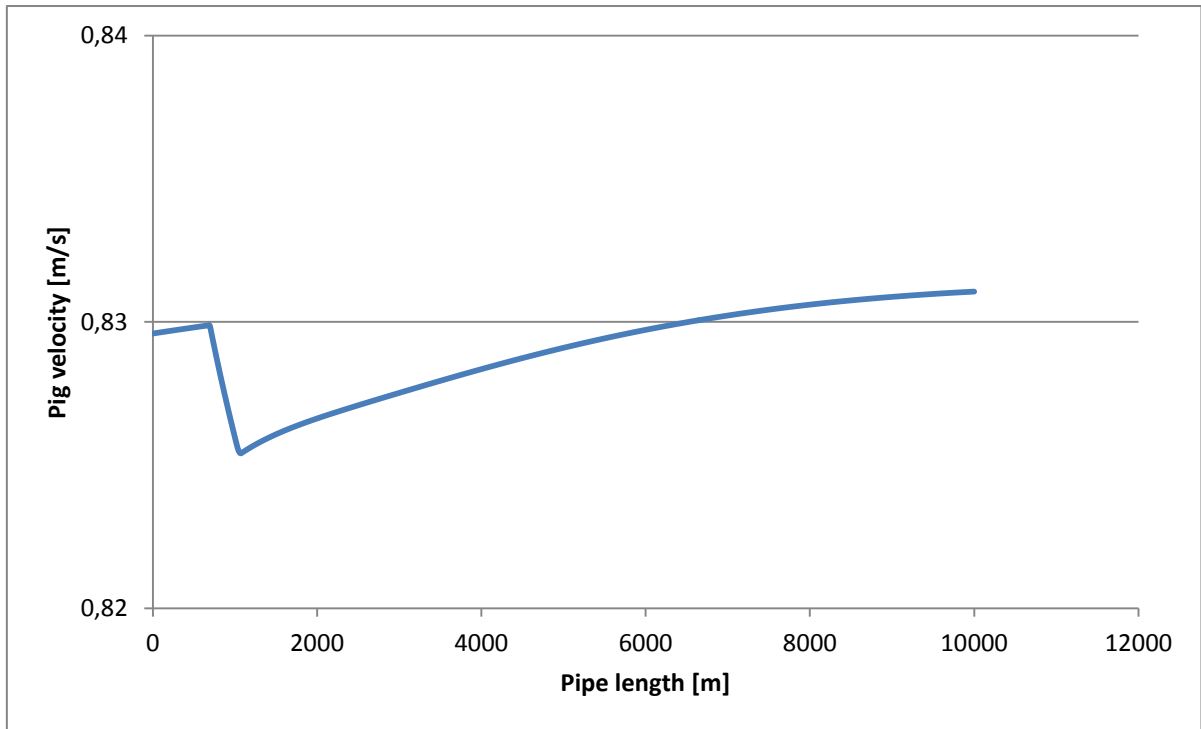


Figure 27: Pig velocity

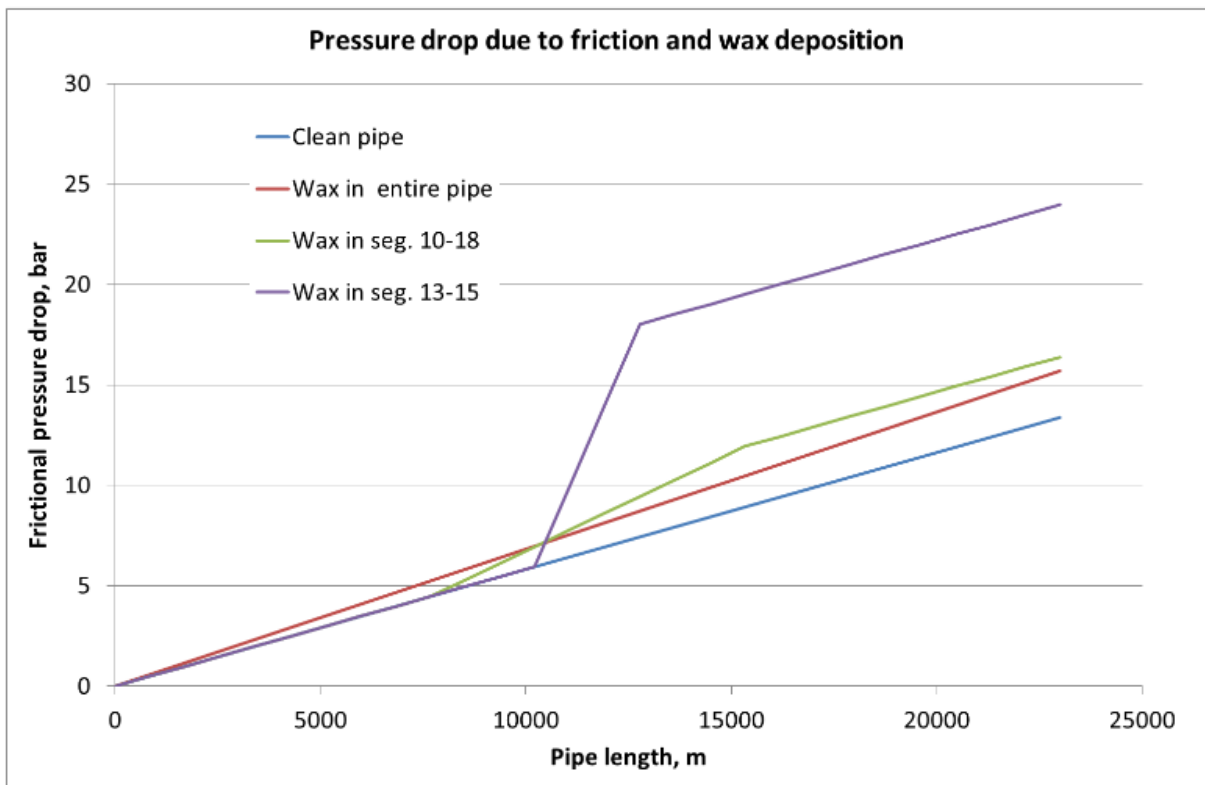


Figure 28: Pressure drop increase for non-evenly distributed deposits (Botne, 2012)

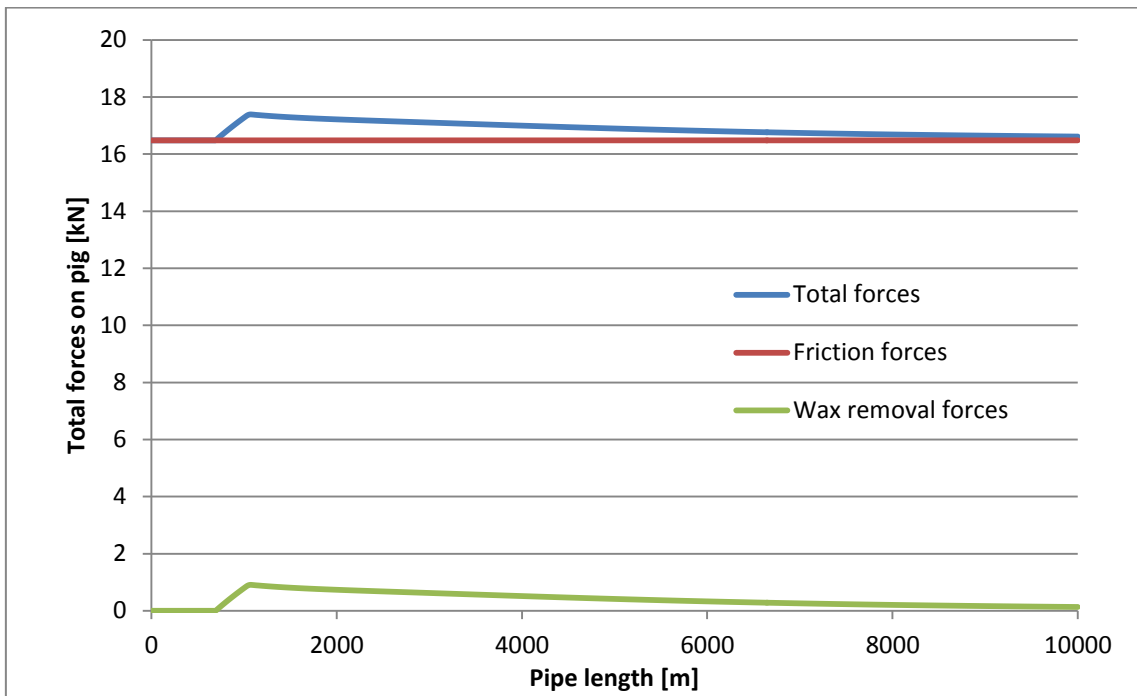


Figure 29: Friction and wax removal forces vs pipe length

Appendices

Appendix A – Calculation of friction for a pig

Pipe ID	0.3	m
E-modulus, E	8	MPa
Disc width, w	0.03	m
Friction coefficient, μ	0.4	
Disc size of pipe ID	105	%
Number of discs, n	6	
Weight of pig, m	50	kg
Oil density	780	kg/m ³
Steel density	7800	kg/m ³
Polyurethane density	1100	kg/m ³

$$\epsilon = \frac{\Delta L}{L_o}$$

$$\epsilon = \frac{(1.03 \cdot 0.3m) - 0.3m}{0.3m} = 0.03$$

$$\sigma_d = \epsilon E$$

$$\sigma_d = 0.03 \cdot 8 \cdot 10^6 Pa = 240\,000 N/m^2$$

$$F_f = N\mu + A_d n \sigma_d \mu$$

Assuming that 1/3 of the volume of the pig is polyurethane and 2/3 is steel. The weight of the pig equals the initial mass minus the weight of displaced oil:

$$\rho_{mix} = \frac{1}{3} \cdot 1100 \frac{kg}{m^3} + \frac{2}{3} \cdot 7800 \frac{kg}{m^3} = 5567 \frac{kg}{m^3}$$

Volume of the pig:

$$V = \frac{m}{\rho_{mix}} = \frac{50kg}{5567kg/m^3} = 0.009 m^3$$

Mass of pig:

$$m_{pig} = 50 kg - \left(780 \frac{kg}{m^3} \cdot 0.009m^3\right) = 43kg$$

Friction equation:

$$F_f = m_{pig}g\mu + 2\pi r w \sigma_d \mu n$$

$$F_f = 43kg \cdot 9.81 \frac{m}{s^2} \cdot 0.4 + 2 \cdot 0.4 \cdot 0.15m \cdot 0.03m \cdot 240000 \frac{N}{m^2} \cdot 0.4 \cdot 6$$

$$F_f = 0.17 kN + 16.3 kN = 16.5 kN$$

Appendix B – Derivation of formula for wax failure stress

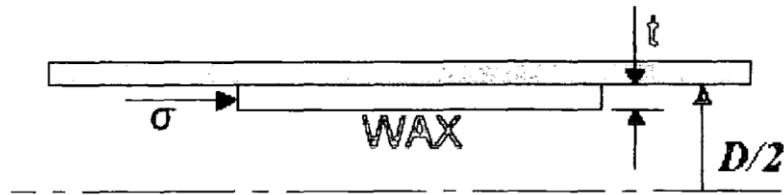


Figure 30: Load model for wax removal (Southgate, 2004).

Where:

σ = Failure stress of wax deposit

D = Pipe diameter

t = thickness of deposit

ΔP = Pressure differential across pig

The force exerted on the pig by the flowing fluid is

$$F_{pig} = \frac{\pi D^2}{4} \Delta P$$

It is assumed that the stress on the wax deposit is compressive and aligned to the pipe axis.

The wax removal force is a product of cross sectional area and the wax failure stress:

$$F_{wax} = \sigma_{wax} \left(\frac{\pi d^2}{4} - \frac{\pi (d - 2t)^2}{4} \right)$$

Equilibrium:

$$F_{pig} = F_{wax}$$

$$\sigma_{wax} \left(\frac{\pi d^2}{4} - \frac{\pi (d - 2t)^2}{4} \right) = \frac{\pi d^2}{4} \Delta P$$

Rearranging:

$$\sigma_{wax} = \frac{\frac{\pi d^2}{4} \Delta P}{\frac{\pi d^2}{4} - \frac{\pi (d - 2t)^2}{4}}$$

Simplifying:

$$\sigma_{wax} = \frac{\Delta P}{\left(\frac{t}{d}\right) \left(4 - \frac{4t}{d}\right)}$$

Reference:

Southgate, J., 2004. Wax Removal using pipeline pigs. PhD's thesis, Durham University, Durham E-Theses Online: <http://etheses.dur.ac.uk/2995/>, June, 269 pp.

Appendix C - Derivation of formula for volumetric flow through an orifice

Bernoulli's equation:

$$P_1 + \frac{1}{2} \rho V_1^2 = P_2 + \frac{1}{2} \rho V_2^2$$

Re-write:

$$P_1 - P_2 = \frac{1}{2} \rho V_2^2 - \frac{1}{2} \rho V_1^2$$

Continuity equation:

$$q = A_1 V_1 = A_2 V_2$$

$$V_1 = \frac{q}{A_1} \text{ and } V_2 = \frac{q}{A_2}$$

$$P_1 - P_2 = \frac{1}{2} \rho \left(\frac{q}{A_2}\right)^2 - \frac{1}{2} \rho \left(\frac{q}{A_1}\right)^2$$

This can be solved for q:

$$q = A_2 \sqrt{\frac{2(P_1 - P_2)/\rho}{1 - \left(\frac{A_2}{A_1}\right)^2}}$$

And:

$$q = A_2 \sqrt{\frac{1}{1 - \left(\frac{d_2}{d_1}\right)^4}} \sqrt{\frac{2(P_1 - P_2)}{\rho}}$$

Beta factor:

$$\beta = \frac{d_2}{d_1}$$

Adding coefficient of discharge:

$$q = C_d A_2 \sqrt{\frac{1}{1 - \beta^4}} \sqrt{\frac{2(P_1 - P_2)}{\rho}}$$

Meter coefficient:

$$C = \frac{C_d}{\sqrt{1 - \beta^4}}$$

This leads to the bypass flow equation:

$$q_{bp} = A_{bp} C_d \sqrt{\frac{2\Delta P}{\rho}}$$

Bypass flow:

$$q_{bp} = C_d \sqrt{\frac{2\Delta P}{\rho}} A_{bypass}$$

Where:

C_d = Discharge coefficient

ρ = Density of fluid

ΔP = Differential pressure across pig

q_{bp} = Volum flow through bypass

A_{bp} = Cross sectional area of bypass

Reference:

Wikipedia, 2014. Orifice Plate. URL: http://en.wikipedia.org/wiki/Orifice_plate. Date accessed: 27.02.14

Appendix G - Calculation of the inside heat transfer coefficient h_i

To calculate the inside heat transfer coefficient h_i both Reynolds number and Prantl number must be calculated. The density, heat capacity, thermal conductivity, viscosity and flow velocity of the oil is used to estimate these dimensionless parameters.

$$Re = \frac{\rho u d}{\mu}$$

Reynolds Number		
u	1.00	m/s
d	0.300	m
ρ	764.6	kg/m ³
μ	1.4282	mPa.s
Re	160611	

$$Pr = \frac{C_{p_f} \mu_f}{k_f}$$

Prantl Number		
C_{p_f}	2416	J/kg·K
μ	1.44	mPa.s
k_f	0.2596	W/m·K
Pr	13.401	

$$Nu_i = 0.0255 Re_i^{0.8} Pr_i^n$$

Nusselt Number	
Re	160611
Pr	13.401
Nu	791.240

When the Nusselt number is known, the inside heat transfer coefficient can be found by using this formula:

$$Nu_i = \frac{h_i d_i}{k_f}$$

Nu	791.240	
d _i	0.300	m
k _f	0.2596	W/m·K
h_i	684.687	W/m ² ·K

Appendix H - Calculation of the outside heat transfer coefficient h_o

Reynolds number is calculated by using the density, flow velocity and the viscosity of the surrounding sea water. d is the outside diameter of the pipe.

$$Re = \frac{\rho u d}{\mu}$$

Reynolds number		
u	0.10	m/s
d_o	0.38	m
ρ	975	kg/m ³
μ	1.88	mPa·s
Re	19699	

$$Pr = \frac{C_{p_f} \mu_f}{k_f}$$

Prantl number		
C_{p_f}	3985	J/kg·K
μ	1.88	mPa·s
k_f	0.6	W/m·K
Pr	12.486	

When Reynolds and Prantl number is calculated, the Nusselt number for external convection is found by using equation 123. C and m are constants that depend on the Reynolds number, see table 12. (Bai & Bai, 2005)

$$Nu_o = CRe_o^m Pr_o^{1/3}$$

Re_o	C	m
4E-01 – 4E+00	0.989	0.330
4E+00 – 4E+01	0.911	0.385
4E+01 – 4E+03	0.683	0.466
4E+03 – 4E+04	0.193	0.618
4E+04 – 4E+05	0.027	0.805

Nusselt number	
Re	19699
Pr	12.486
C	0.193
m	0.618
Nu	201.836

From this, the outside heat transfer coefficient can be found.

$$Nu_o = \frac{h_o d_o}{k_o}$$

External convection h_o		
Nu	201.836	
d	0.3796	m
k	0.65	W/m·K
h_o	345.610	W/m ² ·K

Reference:

Bai, Y. & Bai, Q., 2005. Subsea Pipelines and Risers, Oxford, Elsevier, 919 pp.

Appendix I

Technical Note

MODEL FOR MECHANICAL REMOVAL OF WAX IN PIPELINES

Jon Steinar Gudmundsson

Department of Petroleum Engineering and Applied Geophysics

NTNU

Trondheim

March 2014

Mechanical scrapers (pigs) are used to remove paraffin wax deposits in oil and gas condensate pipelines. To plan and carry out optimal pigging operations it is preferable to know the wax deposit profile along the pipeline and the mechanism(s) of wax removal. The present Technical Note addresses the latter by considering the forces required to remove wax deposits, assuming single phase liquid flow (oil and/or condensate).

The force that moves a scraper pig in a pipeline is the pressure difference (upstream and downstream) of the pig

$$F_p = \Delta p \frac{\pi d^2}{4}$$

where d is the pipeline inner diameter. In non-horizontal situations the gravitational force on the scraping pig (upward or downward) needs to be included.

The opposing forces are the frictional force (between scraper and pipe wall) and the wax removal force(s)

$$F_f + F_{wax}$$

Removal Force

The wax removal force will be considered first. It is proposed here that the wax will be removed when its compressive stress is exceeded - this is the hypothesis. The scraper pig pushes on the deposited wax such that it breaks up and loosens from the pipe wall. It assumes that the adhesive force between the paraffin wax and the pipe wall is included.

Axial stress is given by the general relationship

$$\sigma = \frac{F}{A}$$

having the unit [N/m²]. The compressive strength of a hard paraffin wax has been reported by Hossain et al. (2009) to be 658.4 kPa. Other values reported by the same authors for the paraffin wax were density of 0.7855 kg/m³ and modulus of elasticity of 55.7 MPa. Paraffin wax deposits in pipelines are a mixture of wax and oil/condensate so the quoted compressive strength must be viewed as a maximum value. In lieu of other data, it is proposed here that the compressive strength of paraffin wax deposits in pipelines depends linearly on the oil/condensate content such that

$$\sigma_{wax} = 658(1 - \phi_{oil})$$

where ϕ_{oil} is the volume fraction of oil/condensate. This proposed/assumed linear relationship can be improved if more relevant data are found in the literature, or by experiments.

It would not be surprising that the compressive strength decreases faster with oil volume fraction than linearly. An exponent $n < 1$ should perhaps be added to the $(1 - \phi_{oil})$ term. In the

case that the compressive strength decreases considerably faster, then an exponential term may be more appropriate, for example $\exp(-n\phi_{oil})$.

The wax removal force will be given by the expression

$$F_{wax} = \sigma_{wax} A_{wax}$$

The cross-sectional area of a clean pipe will be

$$A_{pipe} = \frac{\pi}{4} d^2$$

The cross-sectional area of flowing oil/condensate in a pipe with a paraffin wax deposit will be

$$A_{fluid} = \frac{\pi}{4} (d - 2\delta)^2$$

and the cross-sectional area of the wax will be

$$A_{wax} = \pi(\delta d + \delta^2)$$

It follows that the removal force becomes

$$F_{wax} = \sigma_{wax} \pi(\delta d - \delta^2)$$

where δ is the wax thickness. This expression can be improved by including an efficiency factor η , based on laboratory experiments and/or field experience. For simplicity, this factor will not be included in the following text.

An order of magnitude calculation can be carried out assuming a 24 inch (ca. 600 mm) pipeline diameter and a deposit thickness of 6 mm. First, assuming a hard wax deposit (no oil/condensate content).

$$F_w = 658 \cdot \pi \cdot (0.006 \cdot 0.6 - 0.006 \cdot 0.006) = 7.37 \text{ kN}$$

We note (an equation given above) that for a wax deposit containing 50 % volume fraction oil/condensate, the wax removal force will be one-half this value; that is $3.68 \approx 3.7$ kN (assuming a linear effect of oil/condensate volume fraction).

Friction Force

The friction force between the scraper and pipe wall F_f is a difficult quantity to estimate. Fundamentally, the friction force due to gravity between an object moving along a flat wall is given by

$$F_f = \mu_{friction} Mg$$

where $\mu_{friction}$ is the coefficient of friction between to materials, M is the weight of the object and g is the gravitational constant. The coefficient of friction relevant for pipeline scrapers and may lie in the range

$$0.1 < \mu_{friction} < 1$$

Different values are reported in the literature for static and dynamic coefficients. Experiments are required to find out whether the above simple equation for F_f can be used. An order of magnitude can be calculated assuming $\mu_{friction} = 1$ and $M = 50$ kg, resulting in a friction force of $0.495 \approx 0.5$ kN.

We note that the length of the scraper pig is not used in the calculation (the weight, of course, depends on the length and diameter of the scraper pig and the materials of construction). The sealing disks in pigs are typically some sort of hard rubber, resulting in a relatively high coefficient of friction, even greater than 1. Nevertheless, the friction force is much smaller than the wax removal force, in the present example.

The coefficient of friction above is a constant. In reality it may depend on velocity, just as pressure drop due to wall friction in pipes depends on velocity squared, and the friction factor decreases with Reynolds number. Furthermore, the diameter of the hard disks in a scraper pig may be a few percentages larger than the pipeline internal diameter. It can be argued that the frictional force obtained from the simple equation above is the minimum force. An additional force would be that due to the compression/bending of the hard disks.

Force Balance

The force balance for a paraffin wax deposit containing 50 % volume fraction oil/condensate will be

$$F_p = F_f + F_{wax} = 0.5 + 3.7 = 4.2 \text{ kN}$$

the minimum pressure drop across the scraper pig (that drives it forward) will be

$$\Delta p = 4.2 \cdot \frac{4}{\pi \cdot 0.6^2} = 14.8 \text{ kPa} \approx 0.15 \text{ bar}$$

using the full diameter of the pipeline.

The friction force is likely to depend on the scraper pig velocity. Looking for information on such an effect, a paper by Botros & Golshan (2010) was found. It was suggested that the following polynomial could be used for the friction force (based on pigging a gas pipeline)

$$F_f = c_0 + c_1 u_{pig} + c_2 u_{pig}^2$$

$$c_0 = 150 \text{ N}$$

$$c_1 = -4 \text{ N.s/m}$$

$$c_2 = 0.04 \text{ N.s}^2/\text{m}^2$$

Assuming a scraper pig velocity of 2 m/s the polynomial give the friction force as F_f

142 N = 0.142 kN. This value is much lower than the 0.5 kN value calculated/estimated above.

An inspection of the polynomial shows that the c_1 coefficient is negative such that the friction force decreases with velocity, assuming a reasonable velocity range. This seems counter intuitive and needs to be looked at. A model based on fluid flow in a thin layer between a pig and a pipe wall, will depend on both the fluid friction factor and fluid (pig) velocity. The fluid friction factor decreases with velocity (Reynolds number).

By-pass pig

A 600 mm diameter pipeline flowing 750 kg/m^3 oil/condensate at 2 m/s (upstream of scraping pig) has a mass flow rate of 425 kg/s, based on

$$m = \rho u A$$

An orifice-type flow restriction can be modelled by

$$m = C A_2 \sqrt{2 \rho \Delta p}$$

where C is a coefficient (discharge) and A_2 the restricted flow area. The coefficient has typically a value between 0.5 and 0.7. Assuming a mass flow rate 10 % of the total flow rate, a pressure drop of 15 kPa (estimated above) and $C = 0.6$ the effective flow area of the restriction will be 0.0149 m^2 and the diameter 138 mm. This diameter is 23 % of the clean pipeline diameter, which seems too high. A more reasonable value would be 10-15 % of the clean pipe diameter.

Criterion for what percentage by-pass flow would be required for successful pigging is not provided in the present Technical Note. Knowledge about the paraffin wax deposition profile would be an important input in selecting/developing a launching a useful criterion for a scraper pig. One possible criterion could be that the volume fraction wax in the flow downstream of the scraping pig should not be higher than 10 % volume fraction. Slurry flow studies may aid in finding a good criterion.

A by-pass pig should have a non-return valve to make it possible to move it by pressurizing the downstream side; for example, in case the scraping pig gets stuck. A by-pass pig for paraffin wax removal should also have a plate of some sort at the downstream end to distribute the fluid directly to the wall (radial fluid jet to aid in removing deposits). A non-return valve and fluid jet distribution plate would add some pressure drop through the by-pass pig.

Pressure Gradient

A by-pass flow of 42.5 kg/s may ensure that the scarped-off paraffin wax is carried downstream at greater velocity than that of the scarping pig (this is an empirical assumption, for illustration purposes). The average fluid velocity downstream the scarping pig is 10 % greater than 2 m/s (= 2.2 m/s). The velocity gradient in the pipeline will not be the same upstream and downstream of the scraping pig, based on the Darcy-Weisbach equation

$$\Delta p = \frac{f}{2} \frac{L}{d} \rho u^2$$

Upstream the diameter is the full pipeline diameter. Downstream, the diameter is reduced by the paraffin wax deposit. The densities will be slightly different, but not by much because the densities of oil/condensate and paraffin wax are about the same.

The wall friction factor upstream and downstream will be different. This important variable will not be considered in detail in the present Technical Note. Experience indicates that the effective wall roughness of a paraffin wax deposit is much higher than that of a steel pipe. It is proposed here that the effective roughness used in pressure drop/gradient calculations with paraffin wax deposits should be π -times higher than the thickness δ .

Other variable of relevance are temperature and viscosity. Temperature in subsea pipelines decreases exponentially with length according to

$$T_2 = T_u + (T_1 - T_u) \exp \left[\frac{-U \pi d}{m C_p} L \right]$$

The surrounding temperature is T_u and U [W/m².K] the overall heat transfer coefficient (ranges from 15 to 25 for subsea pipelines).

Slurry Flow

The oil/condensate and scraped-off paraffin wax will flow as slurry downstream of the scraping pig. In 1 m length of the example pipeline the volume of the scraped-off wax will be

$$A_{wax} = \frac{\pi}{4} (d - 2\delta)^2$$

$$A_{wax} = \pi(\delta d + \delta^2)$$

$$A_{wax} = \pi(0.006 \cdot 0.6 + 0.006 \cdot 0.006) = 0.0114 \text{ m}^2$$

$$V_{wax} = 0.0114 \cdot 1 = 0.0114 \text{ m}^3$$

Cross-sectional area of fluid (flowing oil/condensate) in a pipeline with a paraffin deposit

$$A_{fluid} = \frac{\pi(d - 2\delta)^2}{4}$$

$$A_{fluid} = \frac{\pi(0.6 - 2 \cdot 0.006)^2}{4} = 0.272 \text{ m}^2$$

Checking the numbers

$$A_{pipe} = \frac{\pi}{4} 0.6^2 = 0.283 \text{ m}^2$$

$$A_{fluid} + A_{wax} = 0.272 + 0.0114 = 0.283 \text{ m}^2$$

Volume fraction paraffin wax in oil/condensate will therefore be

$$\phi_{wax} = \frac{V_{wax}}{V_{wax} + V_{flow}}$$

$$\phi_{wax} = \frac{0.0114}{0.0114 + 0.272} = 0.040$$

In other words, the wax volume percentage is about 4 %. This is quite small so the viscosity of the slurry can be approximated by the Einstein equation

$$\mu = \mu_0(1 - 2.5\phi_{wax})$$

where μ_0 is the viscosity of the oil/condensate (same temperature and pressure) without paraffin wax particles.

Addendum

A detailed literature review was not carried out before the work in the present Technical Note was carried out. The idea was to try to put together a simple wax removal model based on first principles. Subsequently, more detailed studies can be carried out in an academic setting together with inputs (discussions and data) from actors in the oil and gas industry.

As mentioned above, during the writing of the present Technical Note, one paper was found that gave information about the strength and removal of paraffin wax in pipelines (Barros et al. 2005). Therein in a reference was given to Wang et al. (2001). Both papers have a lot of useful information. However, the information was presented in such a way that it is difficult

to make direct comparisons with all aspects of the overall model presented in this Technical Note.

Measured friction forces were reported, but not the compressive strength of the paraffin wax removed. In the Wang et al. (2001) paper the measured forces were reported as dimensionless force referenced to the normal force, without specifying what normal force. In none of the papers was the weight of the scraping pig given (information needed in the model proposed here). Only in one of the papers (Barros et al. 2005) was the mechanical friction coefficient assumed (in the range 0.3 to 0.4).

Concluding Remarks

The model proposed is quite basic/simple and can be used to illustrate how the main parameters affect the pressure required to remove paraffin wax from a pipeline wall. The following comments are offered:

1. The force needed to move a scraper pig is simply the pressure drop between the upstream and downstream ends of the pig.
2. The removal force is proposed to be the compressive strength of the paraffin wax, assumed to include any other additional effect such as adhesive strength.
3. The compressive strength is proposed to be directly proportional to the compressible strength of hard compacted paraffin wax and some function of the volume fraction of oil/condensate in the pipeline wax.
4. The friction force is proposed to be calculated/estimated directly from the fundamental friction-between-solids equation (Coulomb) and hence be proportional to the mechanical friction coefficient and the weight/mass of the scraper pig.
5. Pressure drop through a by-pass pig is proposed to be calculated from a standard flow-through-restriction equation which includes a discharge coefficient.
6. Friction factor for fluid and paraffin wax deposit is proposed to be calculated/estimated based on a sand-grain roughness equal to the multiple of π and the deposit thickness δ . Standard friction factor equation (Haaland) can then to be used.
7. The effective viscosity of the slurry mixture downstream a scraping pig can be estimated from a simple equation (Einstein) based on the fluid viscosity and volume fraction paraffin wax.
8. Literature values (if available), laboratory experiments and field test can be used to obtain more correct values of the parameters in the model.

References

Barros, J.M., Alves, D.P.P., Barroso, A.L., Souza, R.O. & Azevedo, L.F.A. (2005): Experimental Validation of Models for Predicting Wax Removal Forces in Piggging Operations, Proc. 18th International Congress of Mechanical Engineering, November 6-11, 8 pp.

Botros, K.K. & Golshan, H. (2010): Field Validation of a Dynamic Pig Model for an MFL ILI Tool in Gas Pipelines, Proc. 8th International Pipeline Conference, Calgary, Alberta, September 27 – October 1, 12 pp.

Hossain, M.E., Ketata, C. & Islam, M.R. (2009): Experimental Study of Physical and Mechanical Properties of Natural and Synthetic Waxes Using Uniaxial Compressive Strength, Proc. Third International Conference on Modeling, Simulation and Applied Optimization, Sharjah, U.A.E., January 20-22, 5 pp.

Wang, Q., Sarica, C. & Chen T.X. (2001): An Experimental Study on Mechanics of Wax Removal in Pipelines, SPE 71544, SPE Annual Technical Conference and Exhibition, New Orleans, 30 September – 3 October, 8 pp.